R-08-13

Implementation of project Safe in Amber

Verification study for SFR 1 SAR-08

Gavin Thomson, Martin Herben, Pam Lloyd,
Danny Rose, Chris Smith, Ian Barraclough
Enviros Consulting Ltd

March 2008

Svensk Kärnbränslehantering AB
Swedish Nuclear Fuel
and Waste Management Co
Box 250, SE-101 24 Stockholm
Tel +46 8 459 84 00

ISSN 1402-3091
SKB Rapport R-08-13

Implementation of project Safe in Amber

Verification study for SFR 1 SAR-08

Gavin Thomson, Martin Herben, Pam Lloyd,
Danny Rose, Chris Smith, Ian Barraclough
Enviros Consulting Ltd

March 2008

Preface

This report documents an exercise in which AMBER has been used to represent the models used in Project SAFE, a safety assessment undertaken on SFR 1. The AMBER model has been used for radionuclide release calculations in SFR 1 SAR-08 and the document constitutes one of the references used in the safety analysis SFR 1 SAR-08.

Gavin Thomson, Martin Herben, Pam Lloyd, Danny Rose, Chris Smith and Ian Barraclough, Enviros Consulting Ltd have compiled the report.

This document has been reviewed and all comments have been documented in accordance with SKIFS 2004:1.

Stockholm, Mars 2008

Anna Gordon
Project leader, SFR 1 SAR-08

Executive summary

This report documents an exercise in which AMBER has been used to represent the models used in Project SAFE, a safety assessment undertaken on SFR 1.

AMBER has been used to undertake assessment calculations on all of the disposal system, including all disposal tunnels and the Silo, the geosphere and several biosphere modules.

- The near-field conceptual models were implemented with minimal changes to the approach undertaken previously in Project SAFE. Model complexity varied significantly between individual disposal facilities increasing significantly from the BLA to the BTF and BMA tunnels and Silo.
- Radionuclide transport through the fractured granite geosphere was approximated using a compartment model approach in AMBER.
- Several biosphere models were implemented in AMBER including reasonable biosphere development, which considered the evolution of the Forsmark area from coastal to lacustrine to agricultural environments in response to land uplift. Parameters were sampled from distributions and simulations were run for 1,000 realisations.

In undertaking the comparison of AMBER with the various codes and calculation tools used in Project SAFE it was necessary to undertake a detailed analysis of the modelling approach previously adopted, with particular focus given to the near-field models. As a result some discrepancies in the implementation of the models and documentation were noted.

The exercise demonstrates that AMBER is fully capable of representing the features of the SFR 1 disposal system in a safety assessment suitable for SAR-08.

Contents

1 Introduction

Enviros has been supporting SKB in relation to its operation of the L/ILW repository, SFR 1, located near Forsmark.

SKB commissioned Enviros to replicate the existing Project SAFE model /Lindgren et al. 2001/ using the AMBER code. This is part of a programme of support that will aid SKB in responding to the Swedish Regulatory Authorities' review of Project SAFE /SKI and SSI 2004/. As Enviros would use the AMBER code in such supporting studies it is first necessary to replicate the existing Project SAFE model in AMBER, so that the additional impact of any calculations undertaken to illustrate the sensitivity of repository safety and performance to uncertainties or different scenarios can be clearly identified and compared to the Project SAFE results. This will remove the uncertainty that any changes to calculated performance might be due to differences in modelling approaches or assumptions between Project SAFE and the AMBER model.

Chapter 2 provides an overview of SFR 1 and Project SAFE and Chapter 3 describes the software tool AMBER. Chapters 4 to 8 describe the AMBER near-field models (respectively for the Silo, BMA, 1BTF, 2BTF and BLA). Chapter 9 describes the AMBER geosphere model. Chapters 10 to 13 describe the AMBER biosphere models (respectively for reasonable biosphere development, Today's Biosphere, mire and well).

Conclusions are provided in Chapter 14 and references are collated in Chapter 15.

Additional information is also included in Appendix A.

2 SFR 1 and Project SAFE

2.1 Overview of SFR 1

SFR 1 is situated in the northern part of Uppland, close to the Forsmark nuclear power plant and is the central Swedish repository for operational waste from the country's nuclear power plants (NPPs) and for low and intermediate waste (L/ILW) from the Studsvik research reactor. The waste capacity of SFR 1 is approximately 63,000 m^3, and approximately 27,500 m^3 of the waste has already been disposed. In the safety assessment the total radioactivity of all wastes assumed to be disposed at the time of closure is taken to be 10^{16} Bq.

The repository is designed to contain and isolate the waste from the biosphere for an extended period. This is envisaged to be achieved by siting the facility under the seabed, and by a series of engineered barriers that surround the waste. SFR 1 is divided into four types of rock vault connected through a system of tunnels: the Silo; the rock vault for intermediate level waste (BMA); two rock vaults for concrete tanks (1BTF, 2BTF); and the rock vault for low level waste (BLA). The storage vaults are located in the bedrock, approximately 60 m below the seabed, 1 km from the shore. The underground part of the repository is accessed through two tunnels. A schematic of the facility is shown in Figure 2-1.

The bedrock surrounding SFR 1 consists of leptites and fine-grained gneisses, granites and pegmatites /Holmén and Stigsson 2001/. Within the Forsmark area, the bedrock is fractured in a general block-like pattern. The fractures are dominated by steeply and gently dipped fractures which are orientated in NW and NE directions. The structural geological interpretation has been divided into regional and local scales. The regional scale included only the large regional fractured zones whereas the local scale represents the area immediately surrounding the facility.

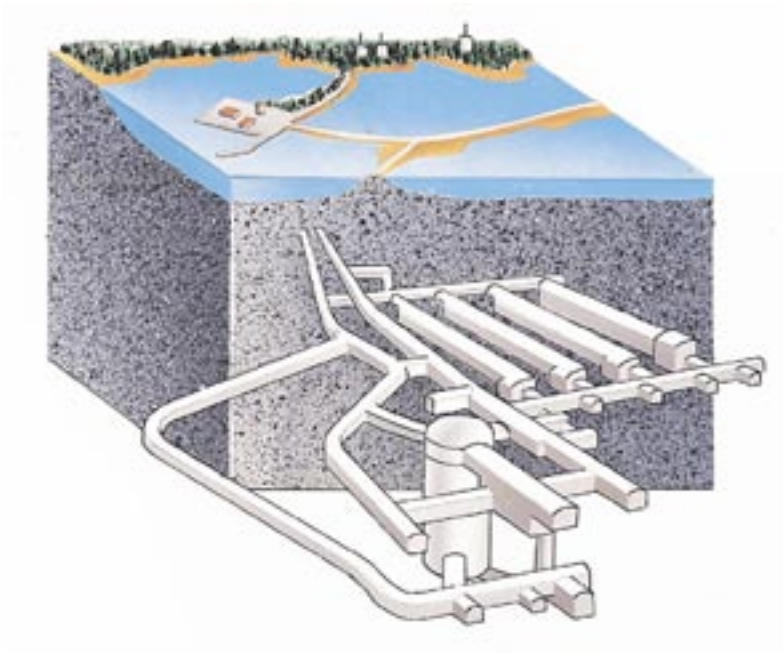

Figure 2-1. *Layout of SFR 1.*

Four local fracture zones are found in the immediate vicinity of the facility, numbered 3, 6, 8 and 9. These zones are sub-vertical. In addition, there are two regional zones near the facility: the sub-horizontal zone H2 and the sub-vertical Singö zone. Zone 6 crosses four of the repository tunnels (1BTF, 2BTF, BLA and BMA); Zone H2 is oriented sub-horizontal beneath the facility, and the other local zones are situated around the facility.

Groundwater flows within the open fractures in the rock mass and the bulk hydraulic conductivity of the rock depends on the properties of a large number of interconnected open fractures. Consequently, the hydraulic conductivity of a certain volume of rock depends on the fracture system inside the volume studied. Since the properties of the fracture system vary within the space, the hydraulic conductivity will be site-dependent and at the same time dependent on the direction of the groundwater flow. Since the conductivity of the rock depends on the properties of the fracture system (for example how fractures are connected within the space) the conductivity will also be dependent on scale.

SFR 1 is located beneath the Baltic sea bed on the eastern Swedish coast. The Baltic Sea is one of the largest brackish water seas in the world and came into existence after the last ice age. The Baltic Sea is connected to the North Sea through two narrow straits with only 8 and 17 m depth. The sea consists of a series of rather shallow basins, separated by sills. The area of the Baltic Sea is 377,400 km^2. The mean water depth has been estimated to 56 m /Kautsky 2001/.

The area local to SFR 1 is a brackish water coastal ecosystem, which is part of Öregrundsgrepen. The pelagic community comprises phytoplankton, bacterioplankton, zooplankton and fish. On shallow soft bottoms the vegetation is dominated by vascular plants. Bottom fauna peak at depths from 2 to 4 m with a high contribution of filter feeders, herbivores and detrivores (which dominate at depth). The most common species of fish in Öregrundsgrepen are herring, roach and perch, followed by ruffe, smelt, fourhorn sculpin, sprat and cod. Conditions are favourable for sea birds, the most common are goldeneyes, tufted ducks, gooseanders, mute-swan, mallards and eider-ducks. The sea eagle is also a frequent visitor in the area and seals are occasional visitors in Öregrundsgrepen /Kautsky 2001/.

The area around SFR 1 is strongly influenced by shore line displacement. A result of the ice melting at the end of the last glacial period is that both glacio-isostatic land uplift and a rise in sea level have resulted in shore line displacement. The present rate of shore line displacement has been estimated to be approximately 0.6 cm/y /Påsse 1997/. Along the coastal areas new lakes are continuously formed as the land rises. New surface water catchments develop, and within these catchments both rivers and lakes form /Kautsky 2001/.

The surrounding land, i.e. the Forsmark area, comprises large areas of wetland and coniferous forest on moraine. The area is situated on the border of two different landscapes: forests typical of this part of Sweden and the coasts and archipelagos of the Baltic Sea. The calcareous moraine is an important contribution to the rich flora and calcareous influenced Chara-lakes. The soils on the flat peneplain are naturally rich in nutrients, but the soils in the areas closer to the coast are thinner, supporting less agricultural activity /Kautsky 2001/.

Forests are the dominating land class covering ca 71% of the area, cultivated fields represent 11%, pastures and meadows ca 3% and the rest (urban areas and other land) totals ca 15%. The amount of arable land has decreased over the years. Today Östhammar municipality has c 17,200 ha cultivated land and c 2,500 ha pastures and meadows. There are no farms close to SFR 1.

Östhammar municipality is quite small and most of the inhabitants live in urban areas. The greatest population density in the municipality is in the south-west, because of the nearness of the urban areas of Uppsala and Arlanda/Märsta. The coastal area of Östhammar municipality has many visitors in the summer and many summer cottages are located close to the Baltic Sea. However, the population density for rural areas is more relevant to the SFR region than that of urban areas. The area nearest to SFR (the parish of Forsmark) has been reported to have a very low population density of only 1.1 inhabitant per km^2 /Kautsky 2001/.

2.2 Swedish radioactive waste regulations

Work with radioactive substances is regulated in Sweden by the Radiation Protection Act. The licensing authority is the Swedish Radiation Protection Authority (SSI – Statens strålskydds-institut), who are authorised to issue regulations and conditions.

There were no specific regulations for final storage of radioactive waste at the time of the licensing of SFR 1, which went into operation in 1988. The facility was therefore controlled under radiation protection regulations for radiological activities at nuclear installations and under regulations concerning release restrictions for radioactive substances applicable to nuclear power plants. Relevant parts of these regulations were utilised as a basis for the radiological design of SFR 1.

Subsequently regulations have been issued which are applicable to final repositories for radioactive waste. SKI FS 1998:1 sets forth the Swedish Nuclear Power Inspectorate's (SKI – Statens kärnkraftinspektions) "Regulations Concerning Safety in Certain Nuclear Facilities". SSI's regulations on the protection of human health and the environment in connection with releases of radioactive substances from certain nuclear facilities are contained in SSI FS 2000:12. Both regulations are applicable during the operating phase of a facility for final disposal of nuclear waste.

For long-term safety SSI has issued "Regulations on the Protection of Human Health and the Environment in Connection with the Final Management of Spent Nuclear Fuel and Nuclear Waste" (SSI FS 1998:1). The regulations entered into force on 1 February 1999. This means that the regulations pertaining to site selection, design, etc are not applicable. The present assessment of the facility's long-term safety is nevertheless compared against the relevant criteria set out in the regulations.

The primary long-term protection criterion for individuals is specified by SSI in its 1998 regulations as an annual risk of "harmful effects" (defined on the basis of ICRP's concept of detriment, indicating a risk coefficient of 7.3% per Sv) of 10^{-6}, for "a representative individual in the group exposed to the greatest risk". The 2005 guidance indicates that the exposed group should be defined such that the risk to the member of the group at highest risk is no more than a factor of ten higher than that to the member at lowest risk. For an exposed group with a significant number of members, the representative risk would be the arithmetic mean of the risks to individuals in the group.

The SSI's regulations refer to two time periods: the first 1,000 years after closure and the period after 1,000 years, but without clearly specifying a distinction in the assessments needed. The treatment of time periods is elaborated upon in the 2005 guidelines:

- The first 1,000 years is the approximate time period for which a risk analysis can be carried out with high credibility with regard to factors such as climate and biosphere conditions.
- For the period from 1,000 years to 100,000 years (approximately), reporting should be based on quantitative risk analysis, but supplementary indicators should be used to strengthen confidence in the calculated risks. In relation to the period after 1,000 years, the guidelines state: "For longer time periods, the result of the risk analysis should be successively regarded more as an illustration of the protective capability of the repository given certain assumptions."
- Beyond 100,000 years or so, the risk analysis should illustrate the long-term development of the repository's barriers.

For repositories such as SFR – i.e. those not for spent nuclear fuel or other long-lived waste – the risk analysis "should at least cover the time until the expected maximum consequences … have taken place, although at the longest for a period of time up to one hundred thousand years."

The SSI guidelines also cover selection of scenarios, in relation to the handing of climate evolution, future human actions and biosphere conditions, environmental protection and reporting of uncertainties. Risk analysis should include a few possible climate evolutions, which "together illustrate the most important and reasonably foreseeable sequences of future climate states".

It should be noted however, that the regulations specifically require an assessment to include a case based on the assumption that the biospheric conditions remain unchanged throughout.

The SSI regulations require the calculation of the collective dose due to the expected outflow of radioactive substances during a period of 1,000 years after closure. This collective dose calculation should integrate the doses up to 10,000 years after closure. However, no numerical criteria are specified for collective dose. SSI's 2005 guidelines indicate that: "The collective dose need not be reported if the repository concept entails a complete isolation of the spent nuclear fuel or the nuclear waste in engineered barriers during the first thousand years after closure."

The licence conditions for SFR include a requirement for an update of the Safety Report at least every 10 years. In June 2001, SKB submitted an integrated revised safety report and periodic safety review report for SFR called Project SAFE /SKB 2001a/.

It is noted that Project SAFE included the following advances over previous safety studies of SFR /Lindgren et al. 2001/.

- An updated inventory which contained information on the radionuclides in each package.
- Revised hydrogeological calculations of groundwater flow within the repository.
- A more detailed near-field assessment model.
- The inclusion of the far-field in all calculation cases.
- A time dependent biosphere.
- Thoroughly reviewed input data.

2.3 Scenarios and calculation cases from Project SAFE

The aim of the calculation cases in Project SAFE was to consider the expected development in the conditions of the repository, rock and biosphere based on four main scenarios and a number of further variations in the calculation cases of the near-field.

A schematic representation of the calculation cases considered in Project SAFE is shown in Figure 2-2 and further description of them is provided in Table 2-1.

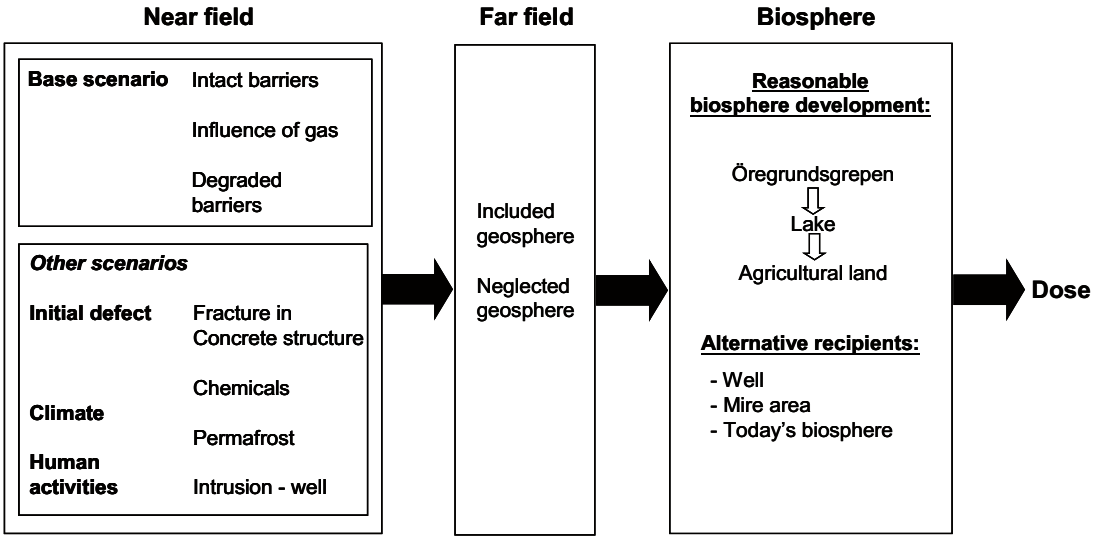

Figure 2-2. *Project SAFE calculation cases /Lindgren et al. 2001/.*

Table 2-1. Summary of calculation cases from Project SAFE /Lindgren et al. 2001/.

Scenario/Calculation case	Description
Base scenario	
Main case (intact barriers)	All technical barriers fulfil the specifications of the construction at closure. Constant properties during the whole time period. Water flow in the near-field influenced by the ongoing land rise. Dose to humans for a reasonable biosphere development that imply release of radionuclides to Öregrunds-grepen during the time period 2,000 AD to 5,000 AD, release to a lake during the period 5,000 AD to 8,000 AD and release to agricultural land during the period 8,000 AD to 12,000 AD. Dose consequence also for the alternatives with release of radionuclides to a well downstream from the repository from 4,000 AD to 12,000 AD, release of radionuclides to a mire area from 4,000 AD to 12,000 AD and for release to Öregrundsgrepen with today's conditions during the whole time period.
Influence of gas	Expelled water containing radionuclides from the near-field barriers due to gas produced in the near-field. Other conditions as in the case "intact barriers". /See Moreno et al. 2001/.
Degraded technical barriers	Conditions as in the case "intact barriers" during the time period 2,000 AD to 3,000 AD. Fractured/degraded barriers in the near-field implies changed flow conditions in the near-field from 3,000 AD until 12,000 AD. Other conditions in the near-field, geosphere and biosphere as in the case "intact barriers".
Other scenario: Initial defects	
Fracture in the concrete structure	Fracture(s) in the concrete barriers at repository closure that increase the water flow through the technical barriers in comparison to the case "intact barriers" in the Base scenario. Other conditions as in the case "intact barriers".
Fracture in the concrete structure and gas	Water containing radionuclides expelled through fracture(s) in the concrete barriers due to gas produced in the near-field. Other conditions as in the case "Fracture in the concrete structure". /See Moreno et al. 2001/.
Chemicals/complexing agents	Considerably poorer sorption in the technical barriers in the near-field. Other conditions as in the case "intact barriers" in the Base scenario.
Chemicals/complexing agents and degraded barriers	Considerably poorer sorption in the technical barriers in the near-field. Other conditions as in the case "degraded technical barriers" in the Base scenario.
Other scenario: Climate	
Permafrost	Frozen repository until 12,000 AD when radionuclide release occurs with the total flow through the different repository parts. Dose consequence with today's biosphere, Öregrundsgrepen.
Other scenario: Human activity	
Well in the repository	A well is sunk in the repository earliest when the shoreline passes by the repository area, i.e. earliest at 3,000 AD. Immediate dose consequence from ingestion. The long term dose consequence caused by the well are changed flow conditions, but otherwise same conditions as in the case "intact barriers" in the Base scenario.

2.4 Conceptual models from Project SAFE

2.4.1 Near-field (Base Scenario)

The near-field is defined as encompassing the vaults, silo and engineered barriers. To take future changes in barrier properties and other conditions into consideration, the base scenario comprises a main case and two further variation cases; each are described above. These variation cases illustrate the consequences of possible, but more uncertain, system processes.

Further to the base scenario and to illustrate the consequences of deviations in the expected properties of the technical barriers, three further variation scenarios are also defined as part of the near-field model: initial barrier defects, climate change (permafrost) and human activity (intrusion).

2.4.2 Main Case (Intact Barriers)

It is firstly assumed that the properties of all technical barriers fulfil the design requirements at closure. That is, no large intersecting fractures are present in the floors, walls and lid of the repository and the compositions of the technical barriers are homogenous. Since it may be possible for damage to occur to waste packages during storage and possible that corrosion could occur, the waste packages are not considered to be barriers.

For assessment purposes, it is assumed that the groundwater will instantaneously flood the repository immediately after closure.

During flooding of the repository, radionuclides will dissolve in the water. The rate at which this is expected to occur is depends on the limitations in the solubility and availability of waste. Once dissolved, the radionuclides will be transferred by advection and diffusion through the waste matrix and surrounding package and barrier materials. As a result, the quantity of radionuclides released from the repository is dependent upon:

- Radionuclide concentration in water.
- Diffusion and sorption properties of the barrier materials (time-independent cement and concrete sorption data is representative of fresh material; having a high pH and ion strength).
- Water flow profiles through the barriers (time-dependent).

Whilst the model assumes no limits of solubility or availability exist for the release of radionuclides into the water, the release from those wastes that are stabilised in bitumen is expected to be almost insignificant unless a network of pores or fractures is formed. Accordingly, the rate of release from the bitumen matrix is estimated to be 1% of the initial radionuclide content per annum.

In order to simulate the expected change in land height, groundwater flow and resultant changed hydrological flow profiles through the repository barriers, the model uses stepwise changes of flow vectors in accordance with the detailed hydrogeological calculations /Holmén and Stigsson 2001/. Until 3,000 AD and based on 2,000 AD hydrogeological calculations, water flow vectors through the repository are expected to be constant. From 3,000 AD until 5,000 AD, stepwise changes are performed for the flow size and direction. However, since only small changes are expected over longer periods. From 5,000 AD stationary flow conditions are assumed to occur.

The influence of Iso Saccharine Acid (ISA) and other complexing agents on sorption through the packages and repository barriers is ignored in the base scenario as data have already been conservatively selected. Despite complexing agents, colloids in the water may also increase the mobility of radionuclides in the near-field. However, owing to the high concentrations of salt, these too are ignored in the base case scenario.

2.4.3 Geosphere

Radionuclides released from the barriers of the repository are carried into the local rock by advection of the flowing water in open rock fractures. The delay (and associated decay) of radionuclides before reaching the biosphere is dependent upon the transport resistance of the rock, which itself is determined by groundwater flow rate, transfer distance and the rate of exchange of radionuclides between the flowing water and rock.

As a consequence of land rise, the shoreline is displaced and the travel distance and groundwater flow profile is expected to change. Although the effect on the release of radionuclides to the biosphere is relatively limited, two variation cases are assessed.

One case (“excluded geosphere”) presents the radionuclide transfer as occurring directly from the near-field into the biosphere. This approach is based on the expectation of a low transport resistance during the first 2,000 years after repository closure and the uncertainty of parameters known to reduce travel times, such as the effect of colloids and microbes.

The second of the two cases ("included geosphere") is based on the time-independent assumption that the influence of rock on the radionuclide release rate into the biosphere can be represented by constant values valid for all repository parts and for the life of the assessment period.

2.4.4 Biosphere

The predicted release points for radionuclides from the geosphere are currently in water about 11 metres deep offshore from Forsmark, under the bed of the Öregrundsgrepen in the Gulf of Bothnia. Gradual uplift of the land in this region due to isostatic rebound from past glaciation is expected to lead to a gradual decrease in sea level, with the release area becoming a lake after 2,000–3,000 years and becoming land after about 6,000–10,000 years. As a base case, it is assumed that this will be agricultural land over this period, but possible release to natural or semi-natural environments were also considered:

- The consequences of release to dry land that is forested were assessed. This possibility is less commonly considered in safety assessments, as the agricultural environment is usually considered to lead to higher doses. However, forests represent a major land use in Scandinavia, and in some circumstances doses from forest ecosystems may be comparable to those from agricultural systems.
- The possibility will also be considered that the release area may remain wetland or mire in this period.

The effects of isostatic rebound could be partially or completely offset (or even reversed) if global sea level were to increase as a result of natural and/or human-driven climate change. This may not be predictable, but might conveniently be linked to the regulatory requirement that the assessment include a case in which biosphere conditions remain unchanged. As well as providing an indication of the time-dependence of releases to the biosphere (in the absence of any confounding changes in biosphere conditions), this case would represent a scenario in which climate-driven rise in sea level cancels out the effect of uplift.

Beyond 10,000 years into the future, glacial cycling is expected to occur, the best current estimate suggesting minor glacial maxima – potentially sufficient to freeze the repository and reduce the ground cover over the waste – preceding a full glacial maximum – with the potential to directly disrupt the waste itself. The effect of glacial maxima occurring at different times from these will also need to be considered, although it is highly unlikely that they would occur within 10,000 years.

No releases of activity from the geosphere will in reality enter the present-day biosphere, and future changes in the biosphere cannot be predicted with any certainty. Reference biospheres are therefore used as a basis for estimating future doses: these are intended to be indicative of the types of biosphere conditions considered likely at different times in the future, not as predictions of the future.

Each set of biosphere conditions was modelled as time-independent, but different conditions were applied to the calculated releases from the geosphere at different times. As noted above, however, calculations were also done for a case in which biosphere conditions remain as at the present day.

To adequately assess the transfer and accumulation of radionuclides in the biosphere (and the resulting dose to biota), four cases are defined:

1. 'Reasonable biosphere development' (based on expected future changes in the biosphere and discharge area).
2. 'Mire area' (to illustrate the effect of uncertainties in discharge area and biosphere development).
3. 'Well' (to illustrate the consequences of release of radionuclides to a future well sunk downstream in the repository area).
4. 'Today's biosphere' (to highlight the influence of the repository independent from changes in the biosphere).

Reasonable biosphere development

The ‘Reasonable’ case is based on four distinct assumptions regarding the time-stepped development of the present Öregrundsgrepen environment: present biosphere conditions will prevail until 4,000 AD, between 4,000 AD and 5,000 AD the water volume and water turn-over will be less that today although the biosphere will continue to act as a coastal receptor; from 5,000 AD to 8,000 AD radionuclides will be released into a newly developed lake, at 8,000 AD wetland and mire areas will be formed, which will be drained and used as agricultural land until 12,000 AD.

Until 5,000 AD, radionuclides released into the Öregrundsgrepen coastal environment are assumed to be distributed between the water phase and suspended material in the water volume, which itself extends into the Baltic Sea. Suspended radionuclides may settle and accumulate in deeper sediments, but may also be re-suspended into the water phase. Uptake into vegetation is assumed only to be from the water column, whilst fish may take up radionuclides both directly from the water and from contaminated particulate and food. Cattle grazing on the shore are assumed to take up the radionuclides by the ingestion of riparian vegetation and water. Human uptake of radionuclides is modelled as occurring via the ingestion of meat, milk and fish from the local area.

From 5,000 AD until 8,000 AD, radionuclides are expected to be released and transferred in the same way in the lake as in the previous coastal environment. It is assumed that radionuclides dissolved or suspended in the water column may leave the system through discharge from the lake. Again, as for the previous environment, radionuclides may be taken up by water vegetation, fish, cattle and human biota. However, in addition to human uptake by ingestion of lake water, it is also assumed that radionuclide uptake may occur through the extraction of lake water, irrigation and subsequent consumption of vegetables and root crops in a garden plot. Further exchanges and transfers are assumed between irrigation water, crop surfaces and internal matter, upper and lower soil regions and the lake. It is assumed that radionuclides may be lost from the system through soil erosion. Additionally, external exposure from radionuclides within soil and inadvertent soil ingestion and inhalation are also included in the assessment as further exposure pathways for human biota.

At 8,000 AD the discharge area becomes agricultural land. Radionuclides supplied by the repository and the deposits accumulated during the earlier coastal and lake periods are expected to be transferred by groundwater into upper soil layers by capillary action, root uptake and by diffusion during dry periods. Similarly, radionuclides may also be drawn down and returned to groundwater by infiltration during wet periods. Radionuclides may be lost from the system by soil erosion and ‘outward’ groundwater flow. Again as during the earlier period, radionuclides are available for root uptake and may be transferred to crops cultivated in the area in the form of cereals, root crops and vegetables. Since part of the area is assumed to be made available as pasturage for cattle, the available exposure pathways to human biota remain as in the earlier period.

Release to a well

The well case illustrates the release of radionuclides to a well that is drilled downstream of the repository area in the future. The consequences of release of radionuclides from the repository to a well downstream the repository during the time period 4,000 AD to 12,000 AD are analysed.

Based on the hydrogeological calculations /Holmén and Stigsson 2001/ it is assumed that all radionuclides released from one repository part exit in this well with a water production rate of 2.37 m^3/day. This was considered sufficient to supply a small agricultural property with 5–10 cows and to also be used for irrigating a small garden plot where vegetables and root crops are grown.

Release to a mire area

It is assumed for this case that the radionuclides are discharged into a mire area from 4,000 AD until 12,000 AD, i.e. these areas do not dry up.

Radionuclides released into the mire area are assumed to be distributed between the water phase and solid material. Losses are assumed to occur by water leaving the system close to the ground surface. It is assumed that peat from the area is used as a soil improver for crop growth and as a household fuel. As a result, exposure pathways to humans are; consumption of cultivated crops, consumption of meat and milk products from cattle raised on cultivated crops, inhalation of peat particles and exhaust gases during peat combustion and external exposure during outdoor occupancy of the mire area.

Release to today's biosphere

The model used for this time-independent case is the same as that used for the first 2,000 years in the reasonable biosphere development case, that is, a coastal model of the current conditions in Öregrundsgrepen.

3 Overview of AMBER

AMBER is a flexible, graphical-user-interface based tool that allows users to build their own dynamic compartmental models to represent the migration, degradation and fate of contaminants in an environmental system. AMBER allows the user to assess routine, accidental and long-term contaminant release. In AMBER, the user may define:

- Any number of compartments.
- Any number of contaminants and associated rates of degradation (both compartment dependent and independent).
- Any number of transfers between compartments.
- Sub-models within larger models.
- Algebraic expressions to represent transfer processes operating between compartments.
- Algebraic expressions to represent the uptake of contaminants by humans and other output quantities of interest.
- Non-linear transfer processes (e.g. solubility-limited leaching).
- Deterministic, probabilistic and time varying parameter values.

Within any given compartment in AMBER, a contaminant is assumed to be uniformly mixed. Each transfer is 'donor controlled', depending directly on the amount of material present in the compartment from which the contaminant is moving (the donor compartment), and can change with time. AMBER allows contaminants to decay or degrade with time into other contaminants, if required. For example, one radionuclide may decay into another.

An AMBER compartment model will usually contain compartments, transfers between compartments and sources providing input of contaminants to compartments.

Mathematically, the amount of contaminant in any compartment is determined by Equation 3-1.

If the total amount of contaminant m in compartment i is I_i^m(moles) then this satisfies:

$$\frac{dI_i^m}{dt} = -\left[\lambda_r^m + \sum_j \lambda_{ij}\right] I_i^m + \lambda_r^{m+1} I_i^{m+1} + \sum_j \lambda_{ji} I_j^m \qquad \text{Equation 3-1}$$

where λ is the exchange rate between compartment i and compartment j (y^{-1}), λ_r^{m+1} is the decay rate of the parent contaminant $m+1$ (y^{-1}), and λ_r^m is the decay rate of contaminant m (y^{-1}).

These equations are linear, so that, for example, if there is twice as much contaminant in the system initially, then the calculated concentrations in the various compartments will all be doubled at each time of interest.

Although the models which can be set up in AMBER are generally limited to those of the linear donor controlled compartment type, this class of models can be applied to a very wide range of problems as a result of the flexibility with which transfers between compartments can be specified. For example, some diffusive-like processes depend upon the concentrations of contaminants in both the donor and receiving compartments, but these can readily be represented in AMBER by including a 'forward' transfer from the donor to the receiving compartment and a 'backward' transfer from the receiving compartment to the donor. The combination of these two transfers will correctly model the net transfer between compartments. Certain non-linear problems, such as those arising from solubility limitations, can also be solved using AMBER.

AMBER has been applied to a wide range of problems concerned with the way that radionuclides and other contaminants move through different parts of the environment. AMBER is used by 59 organisations in 24 different countries. Most of these users have focussed their application on performance assessments of nuclear waste facilities (including surface and deep facilities). Further description of AMBER can be found in the Amber Reference Guide /Enviros and Quintessa 2006/, and verification report /Robinson et al. 2004/. Inter-comparison of the AMBER code is presented by /Maul and Robinson 2002/ and developed further in the white paper /Robinson 2008/.

AMBER has been used in a variety of post-closure safety assessments, and the ability to represent the processes in the conceptual models has been verified according to two directions. The first is via a continuing sequence of verification procedures applied to each new version. These are reported in /Robinson et al. 2004/. Secondly, AMBER has been applied alongside and results contrasted with other assessment tools. These include notably the ISAM Vault Test Case post-disposal assessment /IAEA 2004/, which includes the same processes of advection and dispersion/diffusion which are considered in the post-closure analysis of the SFR. The results obtained from AMBER were in agreement with those obtained using other internationally recognised codes.

The approach followed in this study was to replicate using the AMBER code as closely as possible the conceptual and mathematical models for SFR 1 that were employed in Project SAFE. For the near-field and biosphere, this was relatively straightforward because Project SAFE had adopted compartmental modelling approaches for these sub-systems. So far as was possible, the AMBER models use the same number of compartments, with the same geometry and the same transfers between compartments as Project SAFE. Replicating Project SAFE was less easy for the geosphere, where Project SAFE had employed an analytical approach and, thus, no direct correlation was possible with the compartments in the AMBER sub-model.

So far as was possible, the input data used in the AMBER model were the same as those used in Project SAFE (e.g. inventory data, sorption data, groundwater flow rates, etc). The major sources of information were those produced originally in support of Project SAFE /e.g. Lindgren et al. 2001, SKB 2001b, Holmén and Stigson 2001, Karlsson et al. 2001/. In addition to these sources data for the near-field was obtained from the following sources.

- Radionuclide inventories were provided in spreadsheets by the Project SAFE modelling team.
- Groundwater flow rates were provided in spreadsheets by the Project SAFE modelling team.

Further information specific to the configuration of each component is provided in the following sections with reference to the data used to parameterise the models.

4 Silo model

4.1 Model discretisation

A schematic figure of the Silo model as used in the NUCFLOW calculations in Project SAFE is shown in Figure 2-1 /Lindgren et al. 2001/. This was used as the basis for the development of the corresponding AMBER model. In the AMBER representation of the model, compartments number 37, 38, 39, 40, 41, 42, 48, 50, 51 and 52 were each sub-divided into 5 further compartments (as indicated in the key to Figure 2-1) as was the case for the NUCFLOW simulation. In total this meant that the AMBER model consisted of 94 compartments.

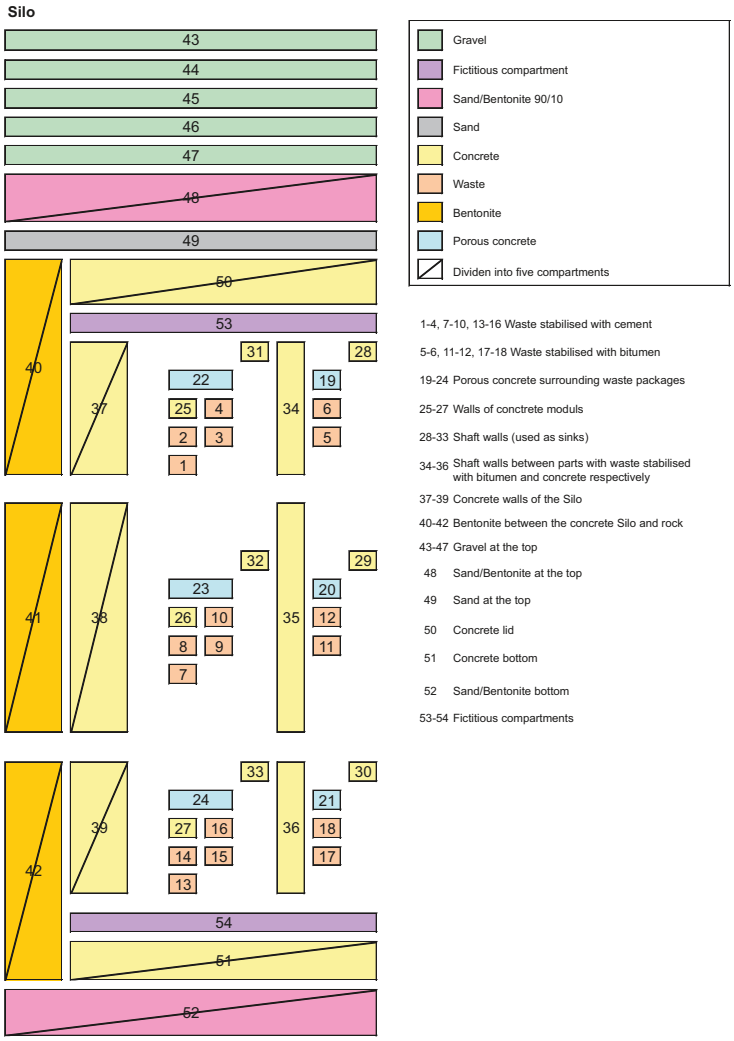

Figure 4-1. *Project SAFE Silo model /Lindgren et al. 2001/.*

4.2 Mathematical representation

The radionuclide transport processes represented in the AMBER model are advection and diffusion.

The advective transport of radionuclide *m* from compartment *i* to *j*, $\lambda^{m}_{ij,\,adv}$ (y^{-1}), is described as follows:

$$\lambda^{m}_{ij,adv} = \frac{Q_i}{Capacity^{m}_{i}} \qquad \text{Equation 4-1}$$

where

Q_i is the groundwater flux through compartment *i* ($m^3\ y^{-1}$),

$Capacity^{m}_{i}$ is the capacity (m^3) of compartment *i* for radionuclide *m*, given by /Lindgren et al. 2001/.

$$Capacity^{m}_{i} = V_i\left(\varepsilon_i + (1-\varepsilon_i)K^{m}_{i\,d}\cdot\rho_i\right) \qquad \text{Equation 4-2}$$

V_i is the volume (m^3) of compartment *i*,

ε_i is the porosity (–) of compartment *i*,

$K^{m}_{i\,d}$ is the distribution coefficient ($m^3\ kg^{-1}$) of radionuclide *m* in compartment *i,*

ρ_i is the particle density ($kg\ m^{-3}$) of compartment *i*.

It was also noted that in some instances the direction of flow between two compartments changed. In order to represent such occurrences it was necessary to model advection between compartments using two transfers (only one of them taking a non-zero value at any one time).

The release of radionuclides from waste stabilised with bitumen was described /Lindgren et al. 2001/ to be represented as occurring at a constant rate over a period of 100 years. In NUCFLOW this was represented using two compartments for the bitumenised waste. The first compartment contained the appropriate disposal inventory for each radionuclide and released the radionuclides using a solubility limit calculated to remain in place over a 100 year period. The second compartment had no initial inventory and received a radionuclide flux from the first.

The radionuclide specific solubility limit was estimated as follows:

$$C^{m}_{i} = \frac{Amount^{m}_{i}}{Q_i\cdot t_{\lim}} \qquad \text{Equation 4-3}$$

where

C^{m}_{i} is the solubility for radionuclide *m* in compartment *i* (moles m^{-3}),

$Amount^{m}_{i}$ is amount of radionuclide *m* in compartment *i* (moles),

Q_i is the groundwater flux from compartment *i* ($m^3\ y^{-1}$),

t_{lim} is period of time over which the release occurs (100 y in this case).

In AMBER this was implemented using an Availability Scheme. An individual scheme was used and the calculation of availability was parameterised as follows:

$$Avail^{m}_{i} = C^{m}_{i}\cdot Capacity^{m}_{i} \qquad \text{Equation 4-4}$$

where

$Avail^{m}_{i}$ is the amount of radionuclide *m* that is available for transfer in compartment *i* (moles).

External advective flows from the near-field (to the geosphere) were also noted to occur and these were represented using the approach described above. During the comparisons of AMBER and NUCFLOW results a discrepancy was noted in the configuration of external flows at the base of the Silo model.

After some correspondence with the Project SAFE modelling team it was realised that in the NUCFLOW calculations the flux of radionuclides from the base of the Silo to the geosphere was calculated on the basis of top-most sand/bentonite compartment, as shown schematically in Figure 4-2.

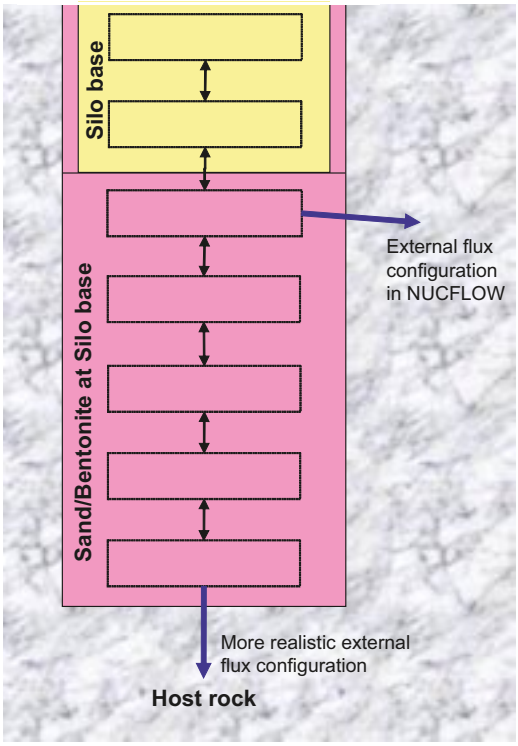

Figure 4-2. *Comparison of configuration of external flows from base of Silo model.*

NUCFLOW also requires a perfect groundwater flow balance and account was also taken of groundwater flows from the geosphere back into the near-field in the NUCFLOW calculations. Such an approach is not required in AMBER and so groundwater fluxes into the AMBER Silo model were neglected.

The diffusive transport of radionuclide m from compartment i to j, $\lambda^{m}_{ij,\,dif}$ (y^{-1}), is described as follows:

$$\lambda^{m}_{ij,dif} = \frac{1}{0.5 \cdot (\mathrm{Res}^{k}_{i} + \mathrm{Res}^{k}_{j}) \cdot Capacity^{m}_{i}} \qquad \text{Equation 4-5}$$

where

Res^{k}_{i} is the diffusive resistance in compartment i in direction k (y m^{-3}),

Res^{k}_{j} is the diffusive resistance in compartment j in direction k (y m^{-3}).

For compartment i, the diffusive resistance in direction k, Res^{k}_{i}, is given by

$$\mathrm{Res}^{k}_{i} = \frac{L^{k}_{i}}{A^{k}_{i} \cdot D^{i}_{e}} \qquad \text{Equation 4-6}$$

L^{k}_{i} is the diffusion length in direction l for compartment i (m),

A^{k}_{i} is the cross-section area for diffusion perpendicular to direction l for compartment i (m^2),

D^{i}_{e} is the effective diffusion coefficient for compartment i (m^2 y^{-1}).

In order to correctly simulate diffusive transfers in AMBER it is necessary to include backwards and forwards transfers for compartments between which diffusion is occurring.

The diffusion of radionuclides from the Silo to the host rock was also considered in Project SAFE and this was represented in NUCFLOW by considering an equivalent flowrate, Q_{eq} (m^3 y^{-1}), (which was estimated by methods described in /Lindgren et al. 2001/). The same approach was used to represent it in AMBER.

4.3 Model parameterisation

The radionuclides considered in the AMBER Silo model are summarised below in Table 4-1. Radionuclide half-lives were taken from /Lindgren et al. 2001/, with the exception of I-129. The half-life of I-129 in /Lindgren et al. 2001/ is stated as 1.6·107 y, whereas in NUCFLOW it is specified as 1.57·107 y, and therefore the latter value was used in the AMBER model.

In general radioactive decay products were not modelled, with the exception of Mo-93 which was assumed to decay to the daughter Nb-93m. Additionally C-14 was assumed to be present in two forms, inorganic and organic, which have identical half-lives. This mirrors the approach adopted in Project SAFE.

Table 4-1. Radionuclides considered and half-lives.

Radionuclide	Half-life (y)
H-3	1.23E+01
C-14	5.73E+03
Cl-36	3.01E+05
Co-60	5.27E+00
Ni-59	7.60E+04
Ni-63	1.00E+02
Se-79	1.13E+06
Sr-90	2.88E+01
Zr-93	1.53E+06
Nb-93m	1.61E+01
Nb-94	2.03E+04
Mo-93	4.00E+03
Tc-99	2.11E+05
Pd-107	6.50E+06
Ag-108m	4.18E+02
Cd-113m	1.41E+01
Sn-126	1.00E+05
I-129	1.57E+07
Cs-135	2.30E+06
Cs-137	3.01E+01
Sm-151	9.00E+01
Eu-152	1.35E+01
Eu-154	8.59E+00
Ho-166m	1.20E+03
Pu-238	8.77E+01
Pu-239	2.41E+04
Pu-240	6.56E+03
Pu-242	3.73E+05
Am-241	4.32E+02

The main sources of information used to configure and parameterise the AMBER Silo model were as follows:

- From the example NUCFLOW input files appended to the SAFE modelling report /Lindgren et al. 2001/, the following information was obtained.
  - Compartmental volumes, V_i, and values of L/A (in x-, y- and z-directions) and material type.
  - Values of material density, ρ_s, porosity, ε_i, and effective diffusivity, D_e, (and distribution coefficient, K_d, see below).
  - Description of diffusive resistances used in transfers between compartments.
  - Compartments from which radionuclides leave the Silo, and the associated groundwater flux, Q.
  - Values of Q_{eq}.
- Information on the distribution of the radionuclide inventory and the groundwater flowfields was taken from the original data used in the Project SAFE calculations provided by the Project SAFE modelling team.

In order to further describe the use of the NUCFLOW input files in configuring AMBER an example input file for inorganic C-14 is included overleaf.

Annotations have been made to the file to explain how the information in the file was used in configuring AMBER to replicate the results. Areas highlighted in bold show markers in the file (e.g. change of information type) and areas highlighted in red have significance for AMBER and are discussed.

The input file has been edited in order to reduce its size by removing sections of it which repeat certain types of information (e.g. compartment properties, source-source connections, source-block connections, block-block connections). These edits are marked as //break//. Therefore, the excerpt included here does not represent an entire input file.

It was noted that discrepancies arose in some compartments that were due to differences in the diffusive resistances used between the compartments. A NUCFLOW output file which lists the diffusive resistances of the compartments was reviewed leading to a limited number of changes being made to the AMBER mode. These are summarised below in Table 4-2.

Table 4-2 Changes to Silo model diffusive resistances.

Connection	Value of diffusive resistance calculated on the basis of NUCFLOW input file (y m^{-3})	Value of diffusive resistance reported by NUCFLOW (y m^{-3}) and used in AMBER
19–20	0.5424	0.54401
19–93	3.544	3.5541
20–21	0.5424	0.54724
21–94	3.544	3.5541
22–93	0.435	0.43508
24–94	0.435	0.43508

```
# PROPER VERSION INPUT DATA FORMAT
#  SILO CALCULATIONS (MP/ML =TODAY())
#
#  Problem Codification: BS2
#  Problem Description:
#
# Nuclide(s): C-14 inorg
#
#  ITYPE    NGROUP    NSINKS    IWFLOW    NSOURC    NBSIZE
ISPSOL
 1 1 3 1 18 0 0
#
#  Flow stream conditions
#  NINFLW    NUTFLW       % if IWFLOW = 1
   10                   1
#
#  Inflow conditions (one line per inflow)
#  QINFW    NBWIN    NBNWIN     % if IWFLOW = 1
       0.00005          5                 1
       0.00015         11                 1
       0.00005         17                 1
       0.044           43                 1
       0.044           44                 1
       0.044           45                 1
       0.044           46                 1
       0.044           47                 1
       0.038           49                 1
       0.23            52                 1
#
#  Outflow conditions (one line per inflow)
#  QUTFW    NBWOUT    NBNWOUT        % if IWFLOW = 1
       0.48825          43
#
# Number of blocks connections and mate
#  NBLOCK    NBCOUP    NMAT
       54 66 10
#
#  Data on materials (one line per material)
#  Material 1 = Waste (Concrete moulds with cement)
#  Material 2 = Waste (Steel with cement)
#  Material 3 = Waste (Bitumen)
#  Material 4 = Porous concrete
#  Material 5 =Construction concrete
#  Material 6 =Bentonite (silo walls)
#  Material 7 =Gravel
#  Material 8 =Sand/bentonite (botten och toppen)
#  Material 9 =Sand (toppen)
#  Material 10 =Water
#  MAT        DENSM          PORM
       1                  2250.0            0.295
       2                  2250.0            0.173
       3                  1030.0            0.119
       4                  2428.6            0.300
                          2529.4            0.150
                          2692.3            0.610
                          2700.0            0.300
                          2666.7            0.250
       9                  2700.0            0.300
       10                  1000.0            1.000
#  Data on time series
#  TINIT      AGEO       RAT       TEND       NTERM       LREAD
       0.00   0.50   1.23   1000.00   90   0
#
#  Data on numerical parameters
#  EPS      EWT       NLOOP       MSPAR
       1.00E-06           1.00E-18          3             1
#
#  Data on group (one set of data per group common for all sources)
#
#  Half-life (y)
#                 ISPSOL                    Solubility Limit (mol m-3)
       1           1                 0
#
# Nuclide: C-14 inorg
#  TAU        CSOLUB       AINV
     5.7300E+03          1.05E+02       8.4724E+00
#
#  CIRF                                                  % if ISPEC = 1
#
#  MAT        DEFM         SKDM                    % one line per material
       1              0.00315          0.200
       2              0.00315          0.200
       3              0.06307          0.000
       4              0.00315          0.200
       5              0.00032          0.200
       6              0.00315          0.000
       7              0.01892          0.001
       8              0.00315          0.000
       9              0.01892          0.001
       10              0.06307          0.000
#
#
```

Radionuclide considered

Solid density (kg m^{-3})

Porosity (-)

Exiting groundwater flux (m^3/y)

Compartment flux exits from

Material names

Effective diffusivity (m^2 y^{-1})

Distribution coefficient (m^3 kg^{-1})

```
#  Data on sources
#  NSBCHA    ISEQ    MAT    IFWATB    VOLSOU    FINVEN    JINVEN
#  IBLOCK    ISSEQ                                      % if ISEQ = 1
#
#  ???                                    EN = 1. One line for each group.
#
#  IBSOUR                                              % if ISEQ = 0
#
                                                      % if IFWATB = 1
#  WBFLOW                                % if IFWATB = 1 and IWINT = 0
#
#  Waste
#  Source    1
  1  0  1  1  702.2400  1.0000000E+00  1
#
  6.8433224E-02
  1
  0
  1.868278E-01
#  Source    2
  1  0  1  1  175.5600  1.0000000E+00  1
#
  1.7108306E-02
  2
  0
  1.868278E-01
#  Source    3
  1  0  2  1  1053.5504  1.0000000E+00  1
#
  4.1786822E-02
  3
  0
  1.868278E-01
#  Source    4
  1  0  2  1  263.3876  1.0000000E+00  1
#
  1.0446705E-02
  4
  0
  1.868278E-01
#  Source    5
  1  0  3  1  0.0001  1.0000000E+00  1
#
  6.2224943E-02
  5
```

Compartment number

Material type

Compartment volume (m^3)

Compartment flow flag (1 = flow considered)

Groundwater flux ($m^3\ y^{-1}$)

```
  0
  5.000000E-05
#
```

//break//

```
#
#  Source    18
  1  0  3  1  617.0864  1.0000000E+00  1
#
  0.0000000E+00
  18
  0
  5.000000E-05
#
#
#  Description of blocks not considered before
#
#  Block i
#  NZ    NY    NX    NBLSP    MAT    IQFLOW
#
                    1 VOLBLK  % one line per compartment if NBLSP = 1
#  IWINT                                                % if IQFLOW = 1
#
#  NODWIN
#
#  Porous concrete in 'inner cylinder' (bitumenised wast
#  Block    19
  1  1  1  0  4  1
  3.8819E-04      9.6177E-05      3.0461E-05      1.9049E+02
  1
#
                                                          -02
  1
#
```

Compartment number

Material type

Compartment flow flag (1 = flow considered)

Compartment volume (m^3)

L/A in z-direction (m^{-1})

L/A in y-direction (m^{-1})

L/A in x-direction (m^{-1})

//break//

```
#
#
#  Block   36
  1  1  1  0  5  0
  1.0000E+05      5.4645E-04      5.4645E-04      7.3200E+01
#
# Concrete silo walls (37-39)
#  Block   37
  1  5  1  0  5  0
  1.0000E+05      9.2957E-04      1.0000E+05      6.8849E+02
#
#  Block   38
  1  5  1  0  5  0
  1.0000E+05      3.0986E-04      1.0000E+05      2.0000E+03
#
#  Block   39
  1  5  1  0  5  0
  1.0000E+05      9.2957E-04      1.0000E+05      6.8849E+02
#
# Bentonite silo walls (40-42)
#  Block   40
  1  5  1  0  6  0
  1.0000E+05      1.2485E-03      1.0000E+05      1.2183E+03
```

Sub-division of compartment into 5 in y-direction

//break//

```
#
#  Codifying the connections
#
#  NSSCO    NSBCO    NBBCO
  9  18  39
#
#  Connection between sources
#  NABCO    ICSEQ    LSCFW    IRADD
#
#  QWATIN                  % if LSCFW is not equal to 0
#
#  ISERNU                  % if IRADD = 1
#
#  XRADD           % if IRADD = 1 and ISERNU = 1 one line per group
#
#  XRADD           % if IRADD = 1 and ISERNU = 0 one line per group
#
#  IBSA    IBSB    ISEQA    ISEQB    % if NABCO > 1 and ICSEQ = 1
#
                                     % if ICSEQ = 0 NABCO*lines
#  WITHIN WASTE
#
#  1 Source-source 1 - 2
     1                0                1                1
     1.868278E-01
     1
     9.131667E-03
     1                2
#
     1                                 1                1
     1
     8.722704E-03
     3                4
#
#  3 Source-source 5 - 6
     1                0                1                1
     5.000000E-05
     1
     1.000000E+12
     5                6
#
#  4 Source-source 7 - 8
     1                0                1                1
     1.868278E-01
     1
     3.043889E-03
     7                8
#  5 Source-source 9 - 10
     1                0                1                1
     1.868278E-01
     1
     2.907568E-03
     9                10
#
#
```

Connection being considered

Groundwater flux ($m^3\ y^{-1}$)

Resistance flag (1 = use value specified here)

Diffusive resistance ($y\ m^{-3}$)

Donor compartment

Receptor compartment

//break//

```
#
#
#  Connection source - block
#
#  IBSOU    IBSB    ISEQC     NABCCO     IRZB     ICRB     IPLUG     IRADD
#  ICOMPB     ICSEQB                      % if NABCCO > 1 and ISEQC =1
#
#  IDCB         % if ISEQC = 0. One value for each connection.
#
# LSCFW QWATIN    % if IFWATB(source term) = 1 and IQFLOW(block) = 1
#
#  XRADD                                    d ISERNU = 0. One line per group.
#  Between waste and conrete wall
#  1 Source-block    2 - 25
     2   25   0   1   1   1   0   1
#
  1
#
  1
  0.00114222934111067
#
# Between cement waste and por
#
#
  1
        18682777
        09109676
#
#  Between bitumen waste - porous c
#  3 Source-block    6 - 19
     6   19   0   1   2   1   0   1
#
  1
  1  0.00005
  1
  6.55058132211069E-05
#
#
```

Connection being considered

Donor compartment

Receptor compartment

Donor resistance flag (1 = use value specified here)

Receptor compartment resistance direction (1 =y)

Receptor compartment resistance flag (1 = included)

Donor diffusive resistance (y m^{-3})

Connection being considered

Donor compartment

Receptor compartment

Donor resistance flag (1 = use value specified here)

Receptor compartment resistance direction (2 =x)

Receptor compartment resistance flag (1 = included)

Groundwater flux direction flag (1 = donor to receptor)

Groundwater flux (m^3 y^{-1})

Donor diffusive resistance (y m^{-3})

//break//

```
#  Between waste in concrete containers - porous concrete
#  10 Source-block    1 - 22
     1   22   0   1   1   0   0   1
#
  1
  -1  0.186827771355237
  1
  100000
#
#
#  11 Source-block    2 - 22
```

Connection being considered

Donor compartment

Receptor compartment

Receptor compartment resistance direction (1 =y)

Receptor compartment resistance flag (0 = ignored)

Donor resistance flag (1 = use value specified here)

Groundwater flux (m^3 y^{-1})

Groundwater flux direction flag (-1 = receptor to donor)

Donor diffusive resistance (y m^{-3})

```
#
#
#  12 Source-block    7 - 23
     7   23   0   1   1   0   0   1
#
  1
  -1  0.186827771355237
  1
  100000
#
#
#  13
#
  1
  1  0.186827771355237
  1
  100000
#
#
```

//break//

```
#
#
#  Connections between blocks not considered as sources
#
#  IBA   IBB   ISEQC   NABCCO   IRZA   IRZB   ICRA    ICRB    IPLUG    IRADD
#
#  IDCA      IDCB                                          % if NABCCO = 1
#
#  ICOMPA   ICOMPB    ICSEQA    ICSEQB     % if NABCCO > 1 and ISQC = 1
#
#  IDCA                                    % if NABCCO > 1 and ISQC = 0
#
#  IDCB                                    % if NABCCO > 1 and ISQC = 0
#  LSCFW      QWATIN                                        )FLOW(B) = 1
          RNU
#  XRADD          % if IRADD = 1 and ISERNU = 0. One line per
#
# Within porous concrete in 'inner cylinder' (bitumenised waste)
#  1 Block-block   19 - 20
  19      20       0       1       2       2       0       0       0       1
    1             1
    -1          4.31722E-02
  1
  5.4240E-01
#
#
                                  2       2       0       0       0       1
#
    -1          4.31722E-02
  1
  5.4240E-01
#
# Between porous concrete and internal concrete walls in 'inner
cylinder' (bitumenised waste)
#  3 Block-block   19 - 28
  19      28       0       1       1       2       1       1       0       0
    1             1
#
#
```

Connection being considered

Donor compartment

Donor & Receptor compartment resistance directions (2 =x)

Donor & Receptor compartment resistance flag (0 = ignored)

Receptor compartment

Groundwater flux direction flag (-1 = receptor to donor)

Groundwater flux (m^3 y^{-1})

Connection diffusive resistance (y m^{-3})

Connection resistance flag (1 = use value specified here)

```
#
#  4 Block-block   20 - 29
  20      29       0       1       1       2       1       1       0       0
    1             1
#
#
#  5 Block-block   21 - 30
  21      30       0       1       1       2       1       1       0       0
    1             1
#
#
# Between porous concrete and concrete walls between 'inner
cylinder' (bitumenised waste) and 'outer cylinder' (cement
conditioned waste)
#  6 Block-block   19 - 34
  19      34       0       1       0       2       1       1       0       0
    1             1
                                  - 35
  20      35       0       1       0       2       1       1       0       0
    1             1
#
#
#  8 Block-block   21 - 36
  21      36       0       1       0       2       1       1       0       0
    1             1
#
#
# Between porous concrete and fiktiv (concrete 'lid' on top of
silo)
#  9 Block-block   19 - 53
  19      53       0       1       0       0       0       0       0       1
    1             1
#
    1         4.31722E-02
  1
  3.5540E+00
#
```

//break//

```
#
```

```
#
# Between concrete in top of silo and fictitious block
#  38 Block-block   50 - 53
  50      53       0       1       0       0       0       1       0       0
    5            1
#
    -1         2.30000E-01
#
# Between concrete in bottom of silo and fictitious block
#  39 Block-block   51 - 54
  51      54       0       1       0       0       0       1       0       0
    1            1
```

```
#
    1         2.30000E-01
#
#
#Data connecting the sinks with the system: one line per sink
# QEQ      IBS      ICS      IRZ      ICRS      ZAFRA
0.00351302855477305     40      5      1      1      0
0.0185983864664455     41      5      1      1      0
0.020251576374574     42      5      1      1      0
```

Equivalent groundwater flux ($m^3\ y^{-1}$)

Compartment

Values of K_d were originally taken from the SAFE radionuclide transport calculations /Lindgren et al. 2001/. However, this resulted in discrepancies for some elements (e.g. Ni, Se) and so the data was reviewed in the NUCFLOW input, which identified some discrepancies, particularly for sand–bentonite. Table 4-3 summarises the values used in the AMBER model. (No sorption is assumed onto bitumen or within water compartments.)

Values which differ from those reported in /Lindgren et al. 2001/ are highlighted in bold (the value reported in /Lindgren et al. 2001/[1] is shown in parentheses in these cases). The reasons for the discrepancies are suggested to be as follows:

- The parameters values describing sorption of inorganic C, Se and Sr onto sand and gravel used in NUCFLOW may have resulted from rounding the values reported in /Lindgren et al. 2001/ to 3 decimal places.
- The methodology stated in /SKB 2001b/ to derive the parameter values for the sand-bentonite mix is a weighted average based on the proportions of materials in the in the backfill (i.e. 90% sand, 10% bentonite). The values in /Lindgren et al. 2001/ seem to be closely based on those reported for sand and gravel, whilst those used in NUCFLOW seem to have been derived using the methodology stated in /SKB 2001b/, with rounding to 3 decimal places (particularly relevant for inorganic C, Se and Sr).

The representation of solubility limits obtained from Equation 4-3 that were used to represent radionuclide release from bitumen are summarised in Table 4-4.

Table 4-3. Sorption coefficients (m^3/kg) used in AMBER models.

Element	Concrete and cement	Gravel and sand	Bentonite	Sand/bentonite 90/10
H	0	0	0	0
C (inorganic)	0.2	**0.001** (0.0005)	0	**0** (0.0005)
C (organic)	0	0	0	0
Cl	0.006	0	0	0
Co	0.04	0.01	0.02	**0.011** (0.01)
Ni	0.04	0.01	0.02	**0.011** (0.01)
Se	0.006	**0.001** (0.0005)	0	**0** (0.0005)
Sr	0.001	**0** (0.0001)	0.001	**0** (0.0002)
Zr	0.5	0.5	0.05	**0.455** (0.5)
Nb	0.5	0.5	0	**0.45** (0.5)
Mo	0.006	0	0	0
Tc	0.5	0.3	0.01	**0.271** (0.3)
Pd	0.04	0.001	0	**0.001** (0.0009)
Ag	0.001	0.01	0	0.009
Cd	0.04	0.01	0.02	**0.011** (0.01)
Sn	0.5	0	0.01	0.001
I	0.003	0	0	0
Cs	0.001	0.01	0.005	0.01
Sm	5	1	0.2	**0.92** (0.9)
Eu	5	1	0.2	**0.92** (0.9)
Ho	5	1	0.2	**0.92** (0.9)
Pu	5	1	1	1
Am	1	1	1	1

[1] Which is also the value reported in /Cronstrand 2005/.

Table 4-4. Concentration limits used for bitumen release from the Silo.

Concentration limit (for 100 year release) (mol m^{-3})	Block 5, 11, 17
H-3	7.13E-03
Inorganic C-14	1.05E+02
Organic C-14	1.17E+01
Cl-36	5.99E+00
Co-60	8.33E+00
Ni-59	1.56E+03
Ni-63	3.46E+02
Se-79	8.99E+00
Sr-90	3.25E+00
Zr-93	3.14E+01
Nb-93m	1.23E-01
Nb-94	4.16E+00
Mo-93	4.08E-01
Tc-99	2.10E+03
Pd-107	1.29E+01
Ag-108m	4.94E-01
Cd-113m	5.60E-03
Sn-126	9.94E-02
I-129	9.37E+00
Cs-135	2.29E+01
Cs-137	3.49E+01
Sm-151	4.46E-01
Eu-152	6.01E-04
Eu-154	3.13E-01
Ho-166m	9.71E-02
Pu-238	3.06E-02
Pu-239	8.34E-01
Pu-240	4.53E-01
Pu-242	1.16E-01
Am-241	4.33E-02

4.4 Comparison of models

Figure 2-2 shows a comparison of the estimated flux from the Silo for AMBER and NUCFLOW. The open symbols are NUCFLOW and the lines are AMBER. For the majority of radionuclide the output times for NUCFLOW and AMBER are identical. However, as NUCFLOW post-process the time series (only print results where there are a significant change) some radionuclides have different output times[2].

[2] In situations in which it was necessary to undertake detailed comparisons of individual radionuclides, the AMBER simulation was re-run using radionuclide-specific output times derived from the corresponding NUCFLOW simulation.

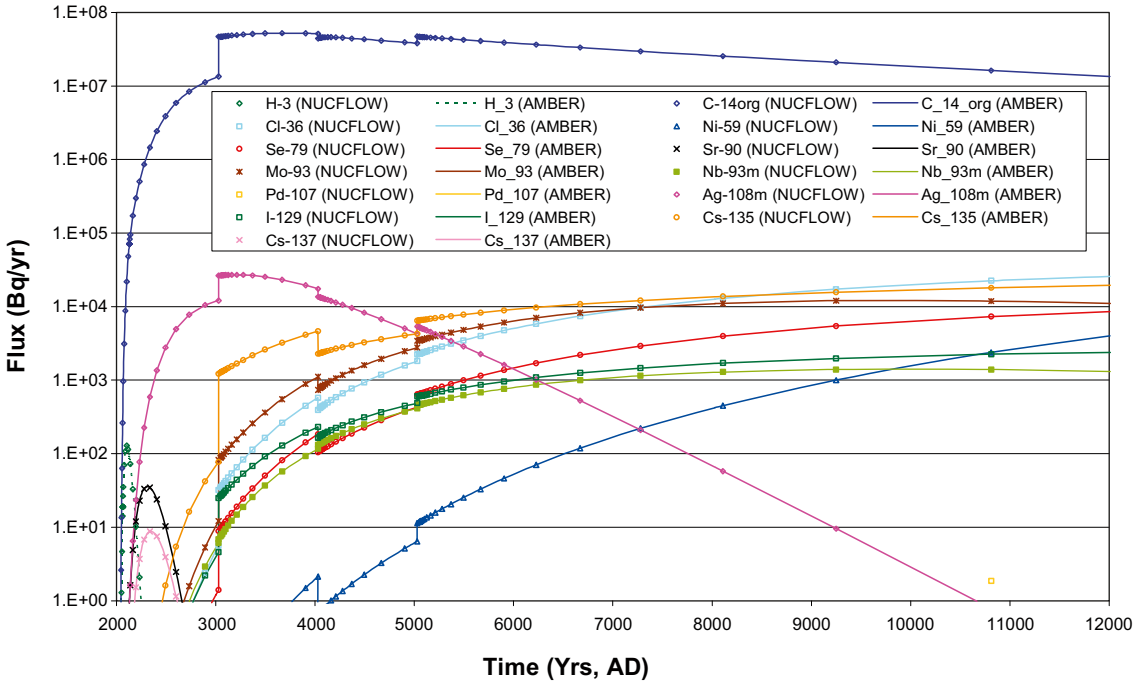

Figure 4-3. *Comparison of Silo near-field flux for selected radionuclides.*

Table 4-5 also summarises the results for each simulation. For each radionuclide reported the first value is the maximum radionuclide flux (Bq y^{-1}) and the second value in parentheses is the time of the maximum radionuclide flux (y). Differences in the models are highlighted in bold. Generally it can be seen that the agreement between the two simulations is very good.

Table 4-5. Summary of comparisons of maximum radionuclide flux and time of maximum for AMBER and NUCFLOW Silo models.

Radionuclide	Maximum radionuclide flux, Bq y^{-1} (time of max, y)	
	AMBER	NUCFLOW
H-3	1.2**90**E+2 (7.2E+1)	1.2**89**E+2 (7.2E+1)
Inorganic C-14	3.61**7**E+0 (1.3E+4)	3.61**6**E+0 (1.3E+4)
Organic C-14	5.22**9**E+7 (1.6E+3)	5.22**8**E+7 (1.6E+3)
Cl-36	3.263E+4 (1.3E+4)	3.263E+4 (1.3E+4)
Ni-59	1.122E+4 (1.3E+4)	1.122E+4 (1.3E+4)
Se-79	1.163E+4 (1.3E+4)	1.163E+4 (1.3E+4)
Sr-90	3.44**1**E+1 (3.1E+2)	3.44**2**E+1 (3.1E+2)
Nb-93m	1.39**3**E+3 (7.2E+3)	1.39**2**E+3 (7.2E+3)
Mo-93	1.198E+4 (7.2E+3)	1.198E+4 (7.2E+3)
Tc-99	3.40**2**E-3 (1.3E+4)	3.40**0**E–3 (1.3E+4)
Pd-107	8.90**6**E+0 (1.3E+4)	8.90**4**E+0 (1.3E+4)
Ag-108m	2.706E+4 (1.2E+3)	2.706E+4 (1.2E+3)
I-129	2.625E+3 (1.3E+4)	2.625E+3 (1.3E+4)
Cs-135	2.31**9**E+4 (1.3E+4)	2.31**8**E+4 (1.3E+4)
Cs-137	8.78**7**E+0 (3.1E+2)	8.78**6**E+0 (3.1E+2)

5 BMA model

5.1 Model discretisation

A schematic figure of the BMA model as used in Project SAFE is shown in Figure 5-1 /Lindgren et al. 2001/. The AMBER model was developed using this configuration of compartments with the exceptions that the fictitious compartments[3] required in NUCFLOW were not required to be included in the AMBER model.

5.2 Mathematical representation

Configuration and parameterisation of the transfers followed the approach described previously for the Silo.

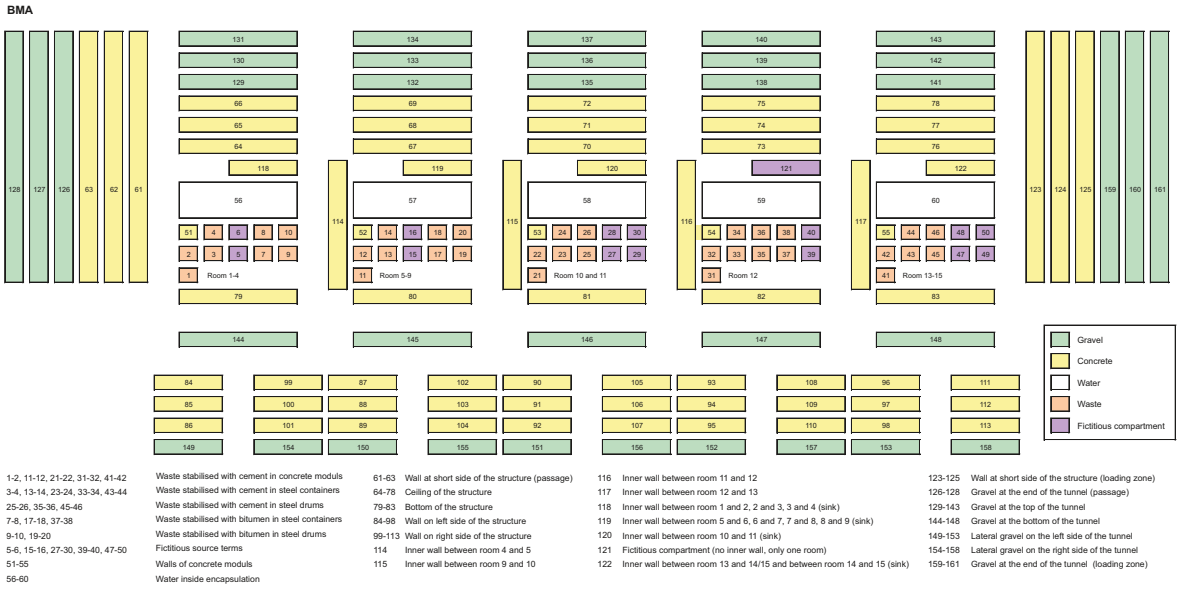

Figure 5-1. *Project SAFE BMA model /Lindgren et al. 2001/.*

[3] In NUCLFLOW, fictitious compartments, compartment numbers 5, 6, 15, 16, 27, 28, 29, 30, 39, 40, 47, 48, 49, 50 and 121, were used to circumvent certain limitations in the code /Lindgren et al. 2001/.

5.3 Model parameterisation

The radionuclides and decay chains considered in the AMBER BMA model are as summarised previously for the Silo. Again the half-life of I-129 was specified as $1.57 \cdot 10^7$ y rather than $1.6 \cdot 10^7$ y used in the SAFE calculations /Lindgren et al. 2001/.

Configuration of the AMBER BMA model followed the same approach as that outlined for the Silo (i.e. using combinations of information from example NUCLFOW input files appended to /Lindgren et al. 2001/, supplemented by information provided by the Project SAFE modelling team). The corrected values of K_d reported in Table 4-3 were also used.

The concentration limits obtained from Equation 4-3 for use in representing radionuclide release from bitumen are summarised in Table 5-1.

Table 5-1. Initial concentration limits used for bitumen release from the BMA.

	Block 7	**Block 9**	**Block 17**	**Block 19**	**Block 37**
Groundwater flux (m^3 y^{-1}) /Lindgren et al. 2001/					
	2.0056E–05	**3.6869E–05**	**5.2368E–05**	**3.23E–05**	**5.00E–05**
Concentration limit (for 100 year release) (mol m^{-3})					
	Block 7	**Block 9**	**Block 17**	**Block 19**	**Block 37**
H-3	8.12872E–04	3.2857E–04	8.1287E–04	3.6962E–04	8.1287E–04
C-14 inorg	1.21381E+01	1.2431E+01	1.2138E+01	1.2138E+01	1.2138E+01
C-14 org	1.34868E+00	1.3812E+00	1.3487E+00	1.3487E+00	1.3487E+00
Cl-36	1.28574E+00	4.1627E–01	1.2857E+00	5.8677E–01	1.2857E+00
Co-60	1.01802E+00	7.9286E–02	1.0180E+00	1.0136E–01	1.0180E+00
Ni-59	1.79404E+02	1.8402E+02	1.7940E+02	1.7962E+02	1.7940E+02
Ni-63	3.95899E+01	3.6853E+01	3.9590E+01	3.6699E+01	3.9590E+01
Se-79	1.93033E+00	6.2490E–01	1.9303E+00	8.8086E–01	1.9303E+00
Sr-90	6.79407E–01	1.6343E–01	6.7941E–01	2.3325E–01	6.7941E–01
Zr-93	3.61250E+00	3.7058E+00	3.6125E+00	3.6172E+00	3.6125E+00
Nb-93m	1.38975E–02	7.1958E–03	1.3898E–02	7.8604E–03	1.3898E–02
Nb-94	4.78886E–01	4.9103E–01	4.7889E–01	4.7933E–01	4.7889E–01
Mo-93	4.70104E–02	4.8111E–02	4.7010E–02	4.6984E–02	4.7010E–02
Tc-99	4.50639E+02	1.4590E+02	4.5064E+02	2.0565E+02	4.5064E+02
Pd-107	2.77668E+00	8.9900E–01	2.7767E+00	1.2672E+00	2.7767E+00
Ag-108m	5.67253E–02	5.6879E–02	5.6725E–02	5.5789E–02	5.6725E–02
Cd-113m	1.15924E–03	1.9052E–04	1.1592E–03	2.7482E–04	1.1592E–03
Sn-126	2.13553E–02	6.9136E–03	2.1355E–02	9.7453E–03	2.1355E–02
I-129	2.01203E+00	6.5143E–01	2.0120E+00	9.1824E–01	2.0120E+00
Cs-135	4.91257E+00	1.5905E+00	4.9126E+00	2.2420E+00	4.9126E+00
Cs-137	7.28611E+00	1.7795E+00	7.2861E+00	2.5384E+00	7.2861E+00
Sm-151	9.46429E–02	2.8076E–02	9.4643E–02	3.9743E–02	9.4643E–02
Eu-152	1.24318E–04	1.9753E–05	1.2432E–04	2.8516E–05	1.2432E–04
Eu-154	6.54316E–02	6.0850E–03	6.5432E–02	8.8723E–03	6.5432E–02
Ho-166m	1.11646E–02	1.1363E–02	1.1165E–02	1.1110E–02	1.1165E–02
Pu-238	4.51991E–03	2.1611E–04	4.5199E–03	2.2133E–04	4.5199E–03
Pu-239	1.23899E–01	6.2910E–03	1.2390E–01	6.4421E–03	1.2390E–01
Pu-240	6.73306E–02	3.4168E–03	6.7331E–02	3.4989E–03	6.7331E–02
Pu-242	1.72691E–02	8.7702E–04	1.7269E–02	8.9808E–04	1.7269E–02
Am-241	6.42532E–03	3.2245E–04	6.4253E–03	3.3021E–04	6.4253E–03

It can be seen from inspection of the data in Table 5-1 that similar effective solubility limits are estimated for compartments 7, 17 and 37 but for compartments 9 and 19 the values differ. In line with the approach adopted in Project SAFE radionuclide-dependent groundwater fluxes were calculated for these compartments (Table 5-2) such that release occurred using a single effective solubility limit.

Table 5-2. Groundwater fluxes required for compartments 9 and 19 to achieve the concentration limit in compartment 7.

Groundwater flux (m^3 y^{-1})	Block 9	Block 19
H-3	1.49025E–05	1.46707E–05
C-14 inorg	3.77590E–05	3.22636E–05
C-14 org	3.77590E–05	3.22636E–05
Cl-36	1.19366E–05	1.47239E–05
Co-60	2.87145E–06	3.21237E–06
Ni-59	3.78168E–05	3.23024E–05
Ni-63	3.43201E–05	2.99073E–05
Se-79	1.19355E–05	1.47227E–05
Sr-90	8.86869E–06	1.10764E–05
Zr-93	3.78213E–05	3.23054E–05
Nb-93m	1.90899E–05	1.82483E–05
Nb-94	3.78039E–05	3.22937E–05
Mo-93	3.77320E–05	3.22455E–05
Tc-99	1.19365E–05	1.47238E–05
Pd-107	1.19369E–05	1.47243E–05
Ag-108m	3.69688E–05	3.17310E–05
Cd-113m	6.05926E–06	7.64871E–06
Sn-126	1.19360E–05	1.47232E–05
I-129	1.19369E–05	1.47243E–05
Cs-135	1.19369E–05	1.47243E–05
Cs-137	9.00456E–06	1.12402E–05
Sm-151	1.09371E–05	1.35482E–05
Eu-152	5.85812E–06	7.40054E–06
Eu-154	3.42871E–06	4.37485E–06
Ho-166m	3.75235E–05	3.21054E–05
Pu-238	1.76284E–06	1.57991E–06
Pu-239	1.87202E–06	1.67754E–06
Pu-240	1.87096E–06	1.67659E–06
Pu-242	1.87239E–06	1.67787E–06
Am-241	1.85024E–06	1.65807E–06

5.4 Comparison of models

Figure 5-2 shows a comparison of the estimated flux from the BMA for AMBER and NUCFLOW. The open symbols are NUCFLOW and the lines are AMBER. For the majority of radionuclide the output times for NUCFLOW and AMBER are identical. However, as NUCFLOW post-process the time series (only print results where there are a significant change) some radionuclides have different output times.

Table 5-3 also summarises the results for each simulation. For each radionuclide reported the first value is the maximum radionuclide flux (Bq y^{-1}) and the second value in parentheses is the time of the maximum radionuclide flux (y). Differences in the models are highlighted in bold. Generally it can be seen that the agreement between the two simulations is very good.

Table 5-3. Summary of comparisons of maximum radionuclide flux and time of maximum for AMBER and NUCFLOW BMA models.

Radionuclide	Maximum radionuclide flux, Bq y^{-1} (time of max, y)	
	AMBER	NUCFLOW
H-3	1.59**1**E+4 (4.3E+1)	1.59**2**E+4 (4.3E+1)
Inorganic C-14	4.045E+5 (2.0E+3)	4.045E+5 (2.0E+3)
Organic C-14	1.61**1**E+8 (1.1E+3)	1.61**2**E+8 (1.1E+3)
Cl-36	2.34**3**E+5 (2.0E+3)	2.34**4**E+5 (2.0E+3)
Ni-59	9.7**53**E+6 (1.3E+4)	9.7**40**E+6 (1.3E+4)
Se-79	7.954E+4 (2.0E+4)	7.954E+4 (2.0E+3)
Sr-90	1.2**72**E+6 (1.1E+2)	1.2**65**E+6 (1.1E+2)
Nb-93m	1.635E+2 (2.0E+3)	1.635E+2 (2.0E+3)
Mo-93	5.100E+5 (2.0E+3)	5.100E+5 (2.0E+3)
Tc-99	5.54**5**E+4 (1.3E+4)	5.54**3**E+4 (1.3E+4)
Pd-107	2.**101**E+3 (1.3E+4)	2.**056**E+3 (1.3E+4)
Ag-108m	6.**399**E+5 (1.0E+3)	6.**400**E+5 (1.0E+3)
I-129	1.4**08**E+4 (2.0E+3)	1.4**10**E+4 (2.0E+3)
Cs-135	1.5**68**E+5 (3.0E+3)	1.5**59**E+5 (3.0E+3)
Cs-137	7.29**1**E+4 (1.3E+2)	7.29**2**E+4 (1.3E+2)

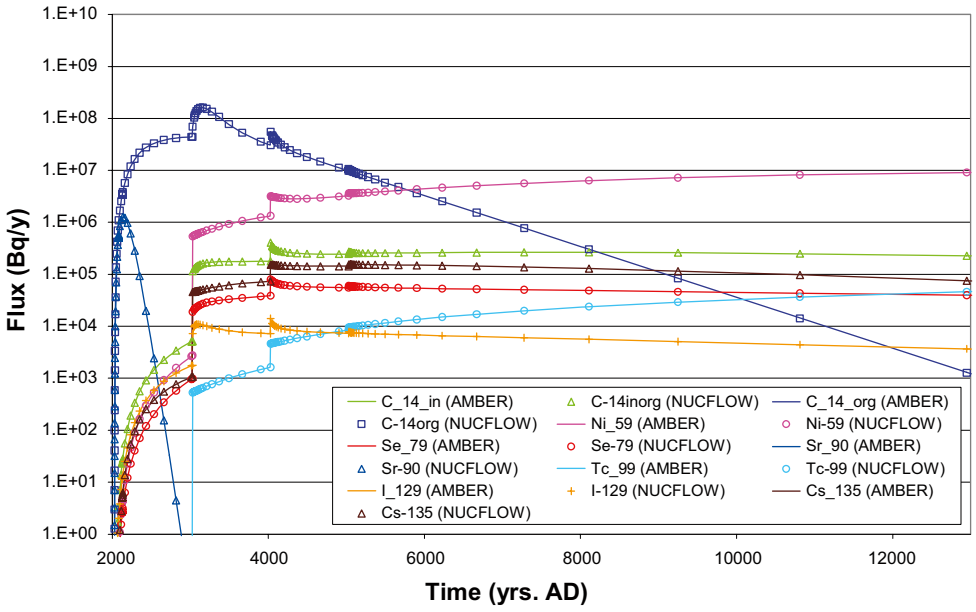

Figure 5-2. *Comparison of BMA near-field flux for selected radionuclides.*

6 1BTF model

6.1 Model discretisation

A schematic figure of the 1BTF model as used in Project SAFE is shown in Figure 6-1 /Lindgren et al. 2001/. The AMBER model was developed using this configuration of compartments with the exception that the fictitious compartments[4] required in NUCFLOW were not required to be included in the AMBER model.

6.2 Mathematical representation

Configuration and parameterisation of the transfers followed the approach described previously for the Silo.

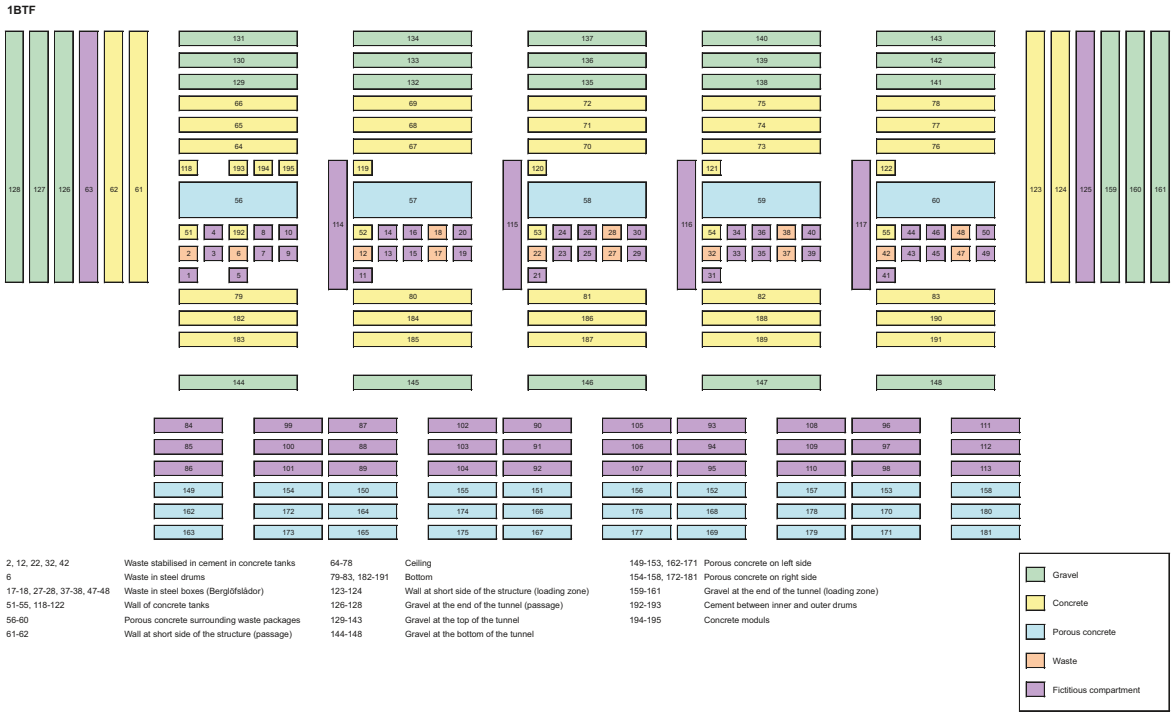

Figure 6-1. *Project SAFE 1BTF model /Lindgren et al. 2001/.*

[4] In NUCLFLOW, fictitious compartments were used to circumvent certain limitations in the code /Lindgren et al. 2001/. Fictitious compartments, shown in Figure 6-1, are compartment numbers 1, 3, 4, 5, 7, 8, 9, 10, 11, 13, 14, 15, 16, 19, 20, 21, 23, 24, 25, 26, 29, 30, 31, 33, 34, 35, 36, 39, 40, 41, 43, 44, 45, 46, 49, 50, 63, 84, 85, 86, 87, 88, 89, 90, 91, 92, 93, 94, 95, 96, 97, 98, 99, 100, 101, 102, 103, 104, 105, 106, 107, 108, 109, 110, 111, 112, 113, 114, 115, 116, 117 and 125.

6.3 Model parameterisation

The radionuclides and decay chains considered in the AMBER 1BTF model are as summarised previously. Again the half-life of I-129 was specified as $1.57 \cdot 10^7$ y rather than the value in /Lindgren et al. 2001/.

Configuration of the AMBER 1BTF model also followed the same approach as that outlined previously (i.e. using combinations of information from example NUCLFOW input files appended to /Lindgren et al. 2001/, supplemented by information provided by the Project SAFE modelling team). The corrected values of K_d reported in Table 4-3 were also used.

It was noted from initial comparisons that the results in certain parts of the 1BTF model did not agree well. From detailed inspection of the NUCFLOW input files it was realised that in two particular compartments of the model an imbalance occurs in the flowfields at 3,000 AD, 4,000 AD and 5,000 AD at the base of the second sub-division of the tunnel as shown below in Figure 6-2 (the compartments whose water flows do not balance are circled).

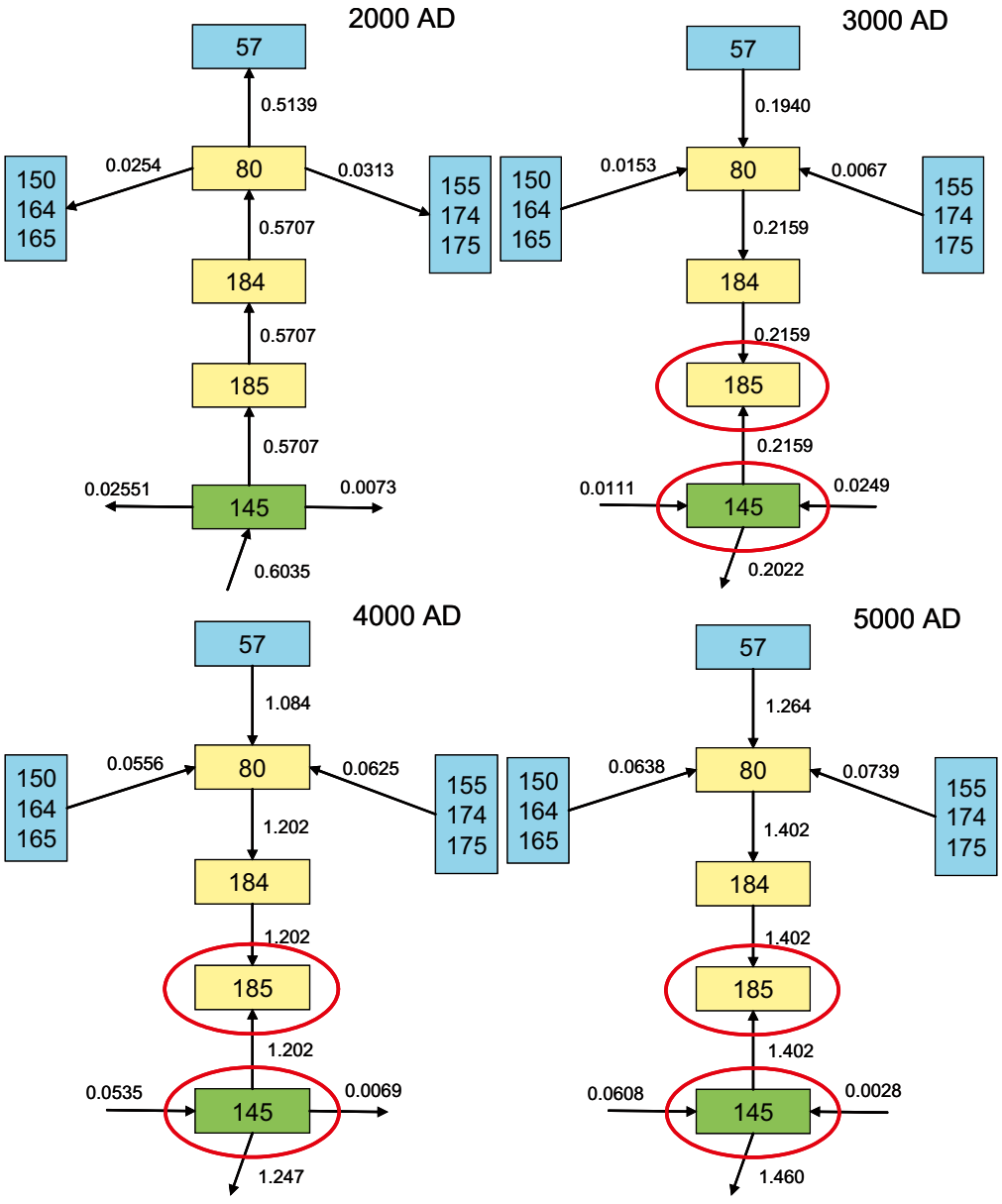

Figure 6-2. *Groundwater flow components (m^3/y) in second sub-division of 1BTF.*

6.4 Comparison of models

Figure 6-3 shows a comparison of the estimated flux from the 1BTF for AMBER and NUCFLOW. The open symbols are NUCFLOW and the lines are AMBER. For the majority of radionuclide the output times for NUCFLOW and AMBER are identical, however, as NUCFLOW simulations are post processed and only relevant changes are printed to the output files some radionuclides have different output times.

Table 6-1 also summarises the results for each simulation. For each radionuclide reported the first value is the maximum radionuclide flux (Bq y^{-1}) and the second value in parentheses is the time of the maximum radionuclide flux (y). Differences in the models are highlighted in bold. Generally it can be seen that the agreement between the two simulations is very good.

Table 6-1. Summary of comparisons for of maximum radionuclide flux and time of maximum AMBER and NUCFLOW 1BTF models.

Radionuclide	Maximum radionuclide flux, Bq y^{-1} (time of max, y) AMBER	NUCFLOW
H-3	1.48**3**E+4 (3.9E+1)	1.48**8**E+4 (3.9E+1)
Inorganic C-14	1.02**5**E+6 (7.2E+3)	1.02**1**E+6 (7.2E+3)
Organic C-14	2.**323**E+8 (1.0E+3)	2.**229**E+8 (1.0E+3)
Cl-36	2.**750**E+4 (3.0E+3)	2.**699**E+4 (3.6E+3)
Ni-59	2.13**8**E+6 (1.3E+4)	2.13**7**E+6 (1.3E+4)
Se-79	1.0**75**E+4 (3.6E+3)	1.0**67**E+4 (3.9E+3)
Sr-90	6.4**04**E+5 (8.8E+1)	6.4**36**E+6 (8.8E+1)
Tc-99	8.**502**E+3 (1.3E+4)	8.**450**E+3 (1.3E+4)
Pd-107	4.24**5**E+2 (1.3E+4)	4.24**2**E+2 (1.3E+4)
Ag-108m	1.91**7**E+5 (1.0E+3)	1.91**4**E+5 (1.0E+3)
I-129	1.**566**E+3 (3.0E+3)	1.5**06**E+3 (3.0E+3)
Cs-135	3.**267**E+4 (3.0E+3)	3.**098**E+4 (3.0E+3)
Cs-137	7.**406**E+3 (1.6E+2)	7.**331**E+3 (1.6E+2)

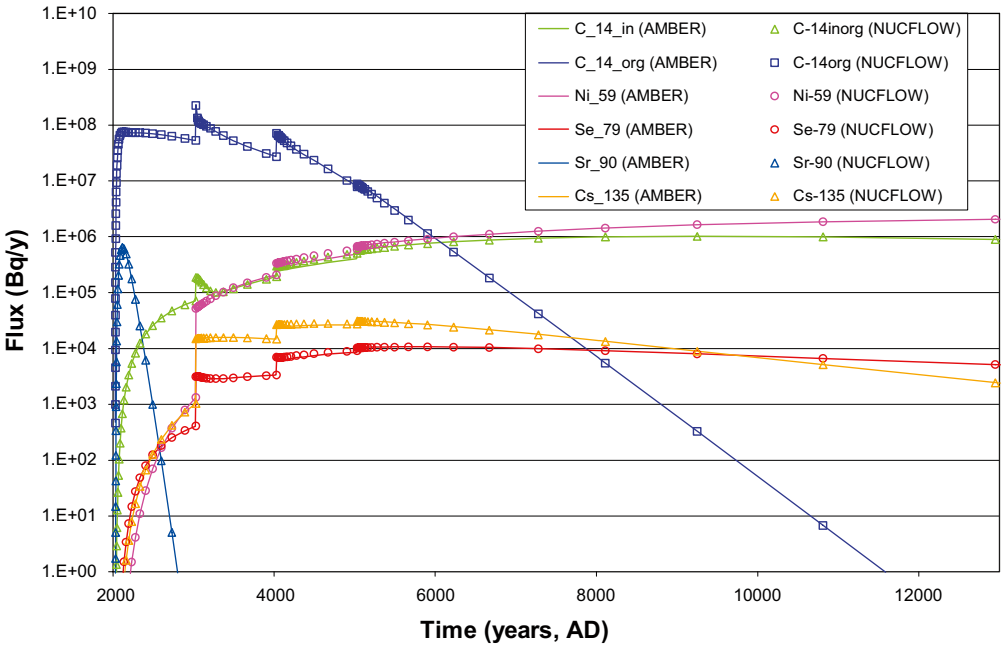

Figure 6-3. *Comparison of 1BTF near-field flux for selected radionuclides.*

7 2BTF model

7.1 Model discretisation

A schematic figure of the 2BTF model as used in Project SAFE is shown in Figure 7-1 /Lindgren et al. 2001/. The AMBER model was developed using this configuration of compartments with the exception that the fictitious compartments[5] required in NUCFLOW were ot required to be included in the AMBER model.

7.2 Mathematical representation

Configuration and parameterisation of the transfers followed the approach described previously for the Silo.

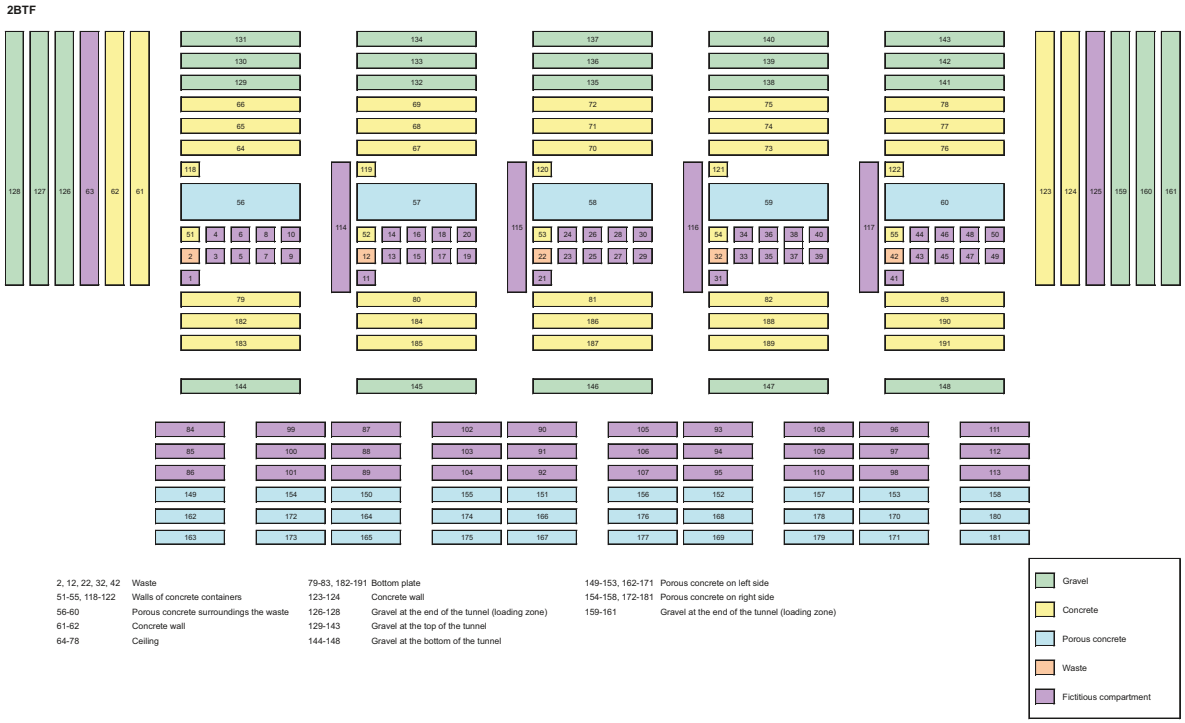

Figure 7-1. *Project SAFE 2BTF model /Lindgren et al. 2001/.*

[5] In NUCLFLOW, fictitious compartments were used to circumvent certain limitations in the code /Lindgren et al. 2001/. Fictitious compartments, shown in Figure 7-1, are compartment numbers 1, 3, 4, 5, 6, 7, 8, 9, 10, 11, 13, 14, 15, 16, 17, 18, 19, 20, 21, 23, 24, 25, 26, 27, 28, 29, 30, 31, 33, 34, 35, 36, 37, 38, 39, 40, 41, 43, 44, 45, 46, 47, 48, 49, 50, 63, 84, 85, 86, 87, 88, 89, 90, 91, 92, 93, 94, 95, 96, 97, 98, 99, 100, 101, 102, 103, 104, 105, 106, 107, 108, 109, 110, 111, 112, 113, 114, 115, 116, 117 and 125.

7.3 Model parameterisation

The radionuclides and decay chains considered in the AMBER 2BTF model are as summarised previously. Again the half-life of I-129 was specified as $1.57 \cdot 10^7$ y rather than the value in /Lindgren et al. 2001/.

Configuration of the AMBER 2BTF model also followed the same approach as that outlined previously (i.e. using combinations of information from example NUCLFOW input files appended to /Lindgren et al. 2001/, supplemented by information provided by the Project SAFE modelling team). The corrected values of K_d reported in Table 4-3 were also used.

It was noted from initial comparisons that the results in certain parts of the 2BTF model did not agree well. From detailed inspection of the NUCFLOW input files it was realised that an imbalance similar to that noted for 1BTF occurs in the flowfields at 4,000 AD and 5,000 AD at the base of the second sub-division of the tunnel as shown below in Figure 7-2 (the compartments which do not balance are circled).

7.4 Comparison of models

Figure 7-3 shows a comparison of the estimated flux from the 2BTF for AMBER and NUCFLOW. The open symbols are NUCFLOW and the lines are AMBER. For the majority of radionuclide the output times for NUCFLOW and AMBER are identical, however, as NUCFLOW simulations are post processed and only relevant changes are printed to the output files some radionuclides have different output times.

Table 7-1 also summarises the results for each simulation. For each radionuclide reported the first value is the maximum radionuclide flux (Bq y^{-1}) and the second value in parentheses is the time of the maximum radionuclide flux (y). Differences in the models are highlighted in bold. Generally it can be seen that the agreement between the two simulations is good.

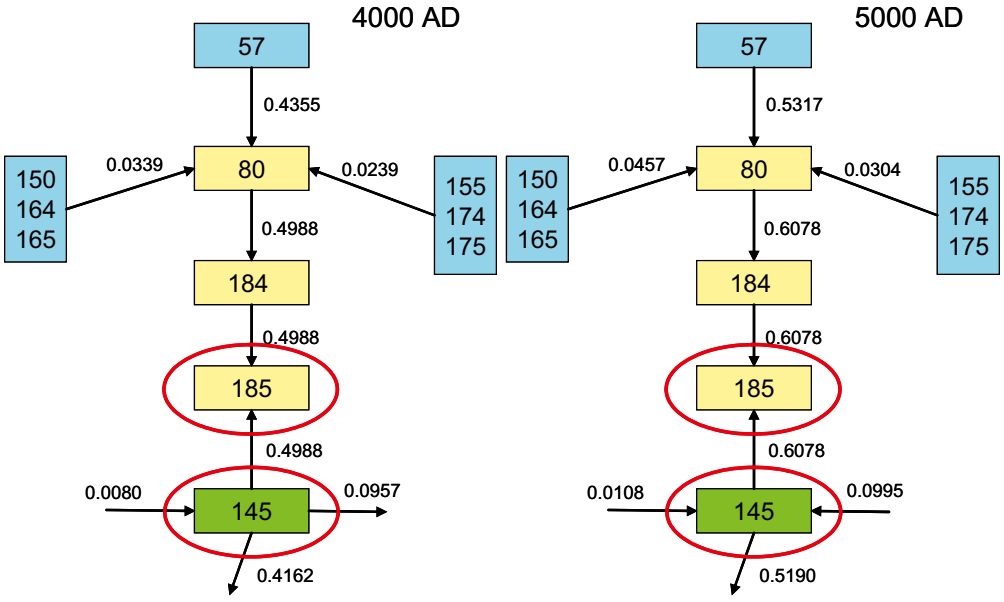

Figure 7-2. *Groundwater flow components (m^3/y) in second sub-division of 2BTF.*

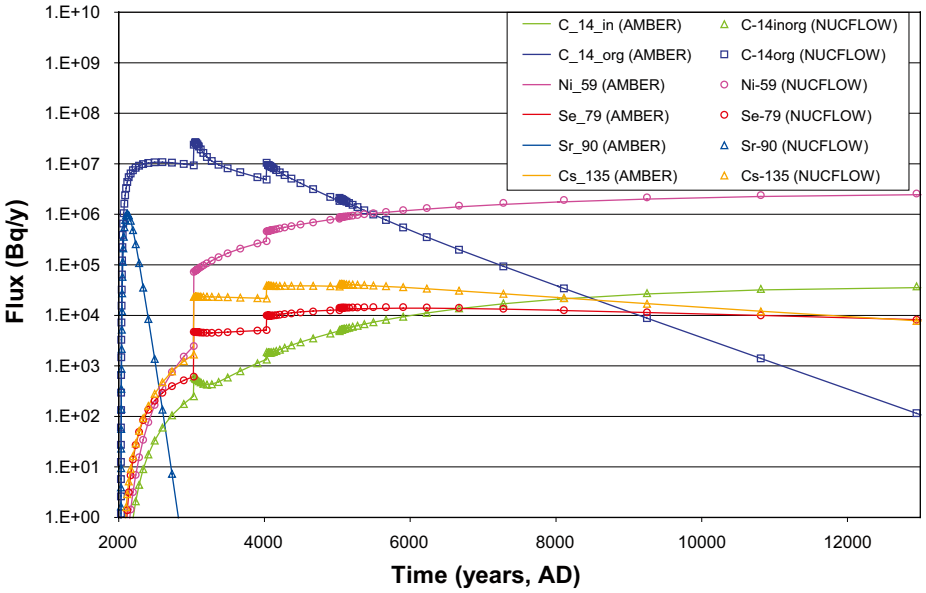

Figure 7-3. *Comparison of 2BTF near-field flux for selected radionuclides.*

Table 7-1. Summary of comparisons of maximum radionuclide flux and time of maximum for AMBER and NUCFLOW 2BTF models.

Radionuclide	Maximum radionuclide flux, Bq y^{-1} (time of max, y)	
	AMBER	NUCFLOW
H-3	2.1**06**E+4 (3.9E+1)	2.1**40**E+4 (3.9E+1)
Inorganic C-14	2.**571**E+4 (1.**2**E+4)	3.**810**E+4 (1.**3**E+4)
Organic C-14	2.64**2**E+7 (1.0E+3)	2.64**0**E+7 (1.0E+3)
Cl-36	3.**722**E+4 (3.**0**E+3)	3.**685**E+4 (3.**5**E+3)
Ni-59	2.**546**E+6 (1.3E+4)	2.**646**E+6 (1.3E+4)
Se-79	1.4**42**E+4 (3.**0**E+3)	1.4**50**E+4 (3.**6**E+3)
Sr-90	1.03**7**E+6 (8.8E+1)	1.03**3**E+6 (8.8E+1)
Tc-99	1.18**6**E+4 (1.3E+4)	1.18**2**E+4 (1.3E+4)
Pd-107	5.**528**E+2 (1.3E+4)	5.**719**E+2 (1.3E+4)
Ag-108m	2.74**5**E+5 (1.0E+3)	2.74**8**E+5 (1.0E+3)
I-129	2.**105**E+3 (3.0E+3)	2.**090**E+3 (3.0E+3)
Cs-135	4.1**74**E+4 (3.0E+3)	4.1**68**E+4 (3.0E+3)
Cs-137	3.74**8**E+4 (1.1E+2)	3.74**9**E+4 (1.1E+2)

8 BLA model

8.1 Model discretisation

The schematic figure of the BLA model used in Project SAFE is shown in Figure 8-1 /Lindgren et al. 2001/ and was used to develop the AMBER model which also represented the BLA using 7 separate compartments.

8.2 Mathematical representation and parameterisation

The mathematical representation of radionuclide release within the BLA is as described for the Silo with the following exceptions:

- No bituminised waste exists within the BLA.
- Diffusive transfer from the BLA to the host rock is not accounted for.

Configuration and parameterisation of the transfers followed the approach described previously for the Silo. However, it should be noted that the diffusion resistances between the waste compartments were not included in the NUCFLOW input files but it is stated in /Lindgren et al. 2001/ that the BLA was considered to be a "stirred tank". Values of L/A were therefore set to an extremely high value (10^{12} m^{-1}) between source compartments in order to minimise diffusive effects on radionuclide transfers. Values of L/A for the connections between the end waste and end gravel compartments were taken from the NUCFLOW input files in /Lindgren et al. 2001/, as described previously.

8.3 Comparison of models

Figure 8-2 shows a comparison of the estimated flux from the BLA for AMBER and NUCFLOW. The open symbols are NUCFLOW and the lines are AMBER. For the majority of radionuclide the output times for NUCFLOW and AMBER are identical, however, as NUCFLOW simulations are post processed and only relevant changes are printed to the output files some radionuclides have different output times.

The agreement for the selected radionuclides is generally very good, as summarised in Table 8-1. In each cell the first number is the maximum radionuclide flux (Bq y^{-1}) and the second number in parentheses is the time of maximum flux (y). Differences between the two models are highlighted in bold.

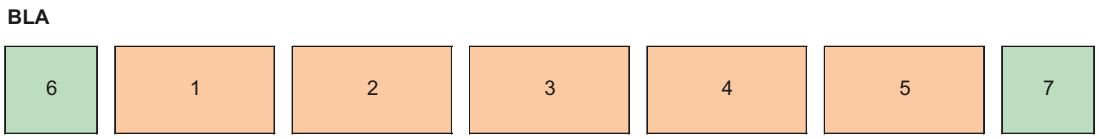

1–5 Source term
6–7 Gravel at the end of the tunnel

Figure 8-1. *Project SAFE BLA model /Lindgren et al. 2001/.*

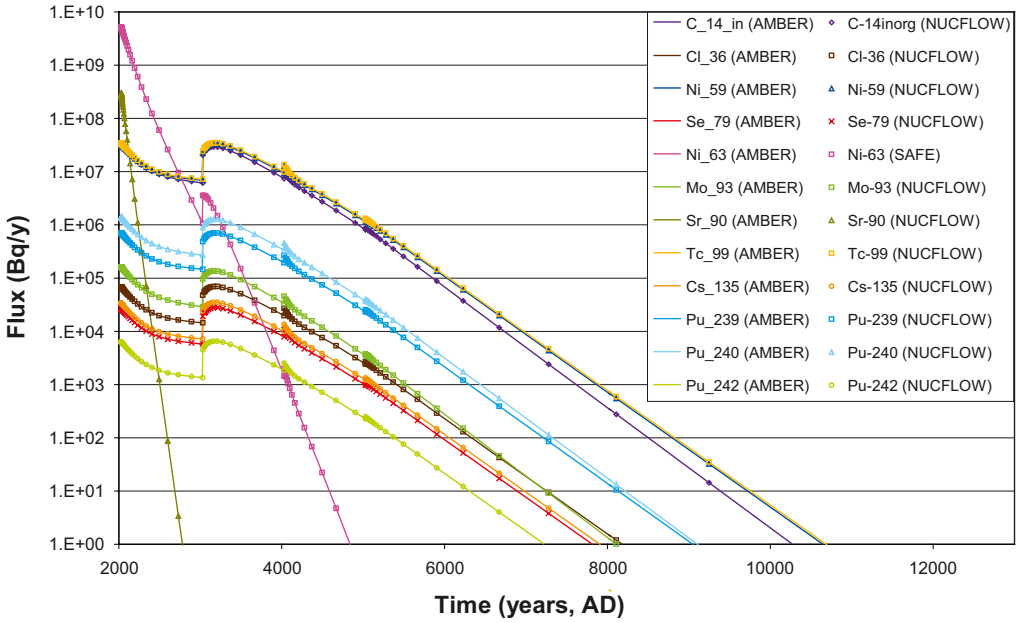

Figure 8-2. *Comparison of the BLA near-field flux for selected radionuclides.*

Table 8-1. Summary of comparisons of maximum radionuclide flux and time of maximum for AMBER and NUCFLOW BLA models.

Radionuclide	Maximum radionuclide flux, Bq y^{-1} (time of max, y)	
	AMBER	NUCFLOW
H-3	5.492E+05 (0)	5.492E+05 (0)
C-14in	3.230E+07 (0)	3.230E+07 (0)
C-14org	2.712E+04 (0)	2.712E+04 (0)
Cl-36	6.973E+04 (1.1E+03)	6.973E+04 (1.1E+03)
Ni-59	3.316E+07 (1.1E+03)	3.316E+07 (1.1E+03)
Se-79	2.794E+04 (1.1E+03)	2.793E+04 (1.1E+03)
Sr-90	2.989E+08 (0)	2.989E+08 (0)
Tc-99	3.482E+07 (1.1E+03)	3.482E+07 (1.1E+03)
Pd-107	6.991E+03 (1.1E+03)	6.990E+03 (1.1E+03)
Ag-108m	1.838E+06 (0)	1.838E+06 (0)
I-129	2.097E+03 (1.1E+03)	2.097E+03 (1.1E+03)
Cs-135	3.495E+04 (1.1E+03)	3.494E+04 (1.1E+03)
Cs-137	3.097E+09 (0)	3.097E+09 (0)

9 Geosphere model

The approach described here is based on guidance on the use of AMBER to represent transport through fractured media /Robinson 2008/. The aim was to ensure AMBER suitably replicates the approach taken by the code FARF31 to model radionuclide transport in a fractured media. FARF31 /Norman and Kjellbert 1990/ is used by SKB to represent radionuclide migration through the geosphere. FARF31 calculates the transport, retardation and radioactive chain decay of dissolved radionuclides within fractured rock and is based on the consideration of a 1-dimesional stream-tube.

9.1 Model discretisation

The geosphere model is represented in AMBER as a two dimensional array of compartments (Figure 9-1). In one dimension, compartments (F1, F2, etc) are linked together to represent the advective flow path along a fracture. The number of compartments in this dimension was chosen as 40 to reduce the effects of numerical dispersion on the simulation. In the perpendicular dimension, compartments (M1, M2, etc) were included to represent parts of the adjacent rock matrix that undergo diffusive exchange (matrix diffusion).

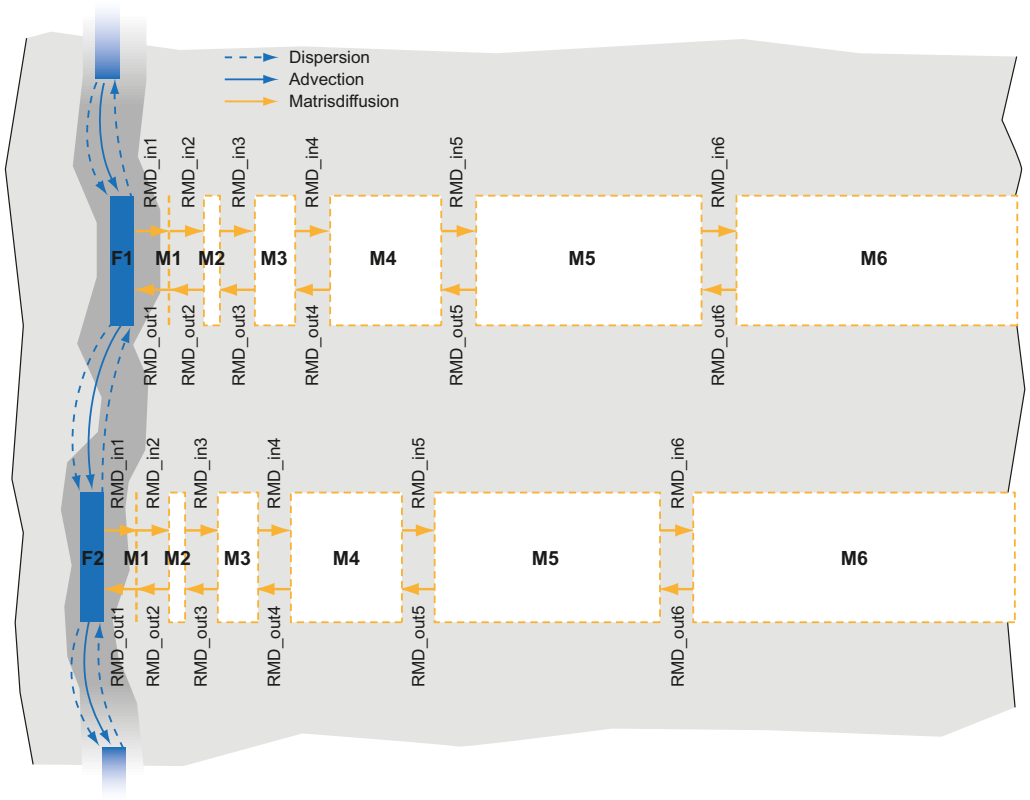

Figure 9-1. *Discretisation of geosphere within AMBER.*

9.2 Mathematical representation

The advective transfer from compartment i to j, $\lambda_{ij,\,Adv}$ (y^{-1}), is given by:

$$\lambda_{ij,Adv} = \frac{v}{R_f L_i} \qquad \text{Equation 9-1}$$

where

v is the average linear groundwater velocity (m y^{-1}),

R_f is the effective retardation within the fracture (–),

L_i is the length of compartment i (m).

The inclusion of effective retardation in the fracture results from considering a thin layer of matrix and so

$$R_f = 1 + a_W d_0 \theta R_m \qquad \text{Equation 9-2}$$

where

a_w is the flow wetted surface area ($m^2\ m^{-3}$),

d_0 is the thickness of the thin layer (m),

θ is the matrix porosity (–),

R_m is the retardation within the rock matrix (–), given by

$$R_m = 1 + \rho \cdot K_d \big/ \theta \qquad \text{Equation 9-3}$$

ρ is the rock matrix bulk density ($kg\ m^{-3}$),

K_d is the distribution coefficient for the rock matrix ($m^3\ kg^{-1}$).

The following relationship was used to determine an approximate value of d_0.

$$d_0 = \sqrt{\frac{2 D_e t_f}{\theta R_m}} \qquad \text{Equation 9-4}$$

where

D_e is the effective matrix diffusion coefficient ($m^2\ y^{-1}$),

t_f is the travel time (y).

A value of 0.0001 m for d_0 was estimated using data for plutonium as this is the most strongly sorbed radionuclide and so requires the finest resolution. This value was used for all radionuclides.

The forward dispersive transfer rate (along the fracture), $\lambda_{ij,\,Disp}$ (y^{-1}), is given by:

$$\lambda_{ij,\,Disp} = \frac{\frac{v \cdot L_{tot}}{R_f \cdot P_e} - \frac{v \cdot L_i}{2 \cdot R_f}}{L_i^{\,2}} \qquad \text{Equation 9-5}$$

where

L_{tot} is the total flow path length (m),

P_e is the Peclet number (–).

The backward dispersive transfer rate, $\lambda_{ji,\,Disp}$ (y^{-1}), is given by:

$$\lambda_{ji,\,Disp} = \frac{\frac{v \cdot L_{tot}}{R_f \cdot P_e} - \frac{v \cdot L_j}{2 \cdot R_f}}{L_j^{\,2}} \qquad \text{Equation 9-6}$$

where
L_j is the length of compartment j (m).

The rate of diffusion from the fracture into the initial matrix compartment, λ_{RMD_in1}, is given by:

$$\lambda_{RMD\_in1} = \frac{2a_w D_e}{R_f d_1}$$ Equation 9-7

where
d_1 is the depth of the initial matrix compartment (m).

The rate of matrix diffusion from compartment j to compartment $j+1$ (i.e. further into the matrix) is given by:

$$\lambda_{RMD\_inj,j+1} = \frac{2D_e}{\theta R_m d_j (d_j + d_{j+1})}$$ Equation 9-8

where
d_j is the depth of the matrix compartment j (m),
d_{j+1} is the depth of the matrix compartment $j+1$ (m).

The rate of diffusion from the initial matrix compartment into fracture, λ_{RMD_out1}, is given by:

$$\lambda_{RMD\_out1} = \frac{2D_e}{\theta R_m d_1^{\,2}}$$ Equation 9-9

The rate of matrix diffusion from compartment $j+1$ to compartment j is given by:

$$\lambda_{RMD\_inj+1,j} = \frac{2D_e}{\theta R_m d_{j+1} (d_j + d_{j+1})}$$ Equation 9-10

9.3 Model parameterisation

The data used in the AMBER geosphere model are shown in Table 9-1. In addition to those data reported below values for K_d and D_e were taken from /Lindgren et al. 2001/.

Table 9-1. Compilation of geosphere data.

Parameter	Value	Reference
Travel time, t_f, (y)	50	/Lindgren et al. 2001/
Peclet number, P_e (–)	10	/Lindgren et al. 2001/
Flow wetted surface area, a_w, ($m^2\ m^{-3}$)	120	/Lindgren et al. 2001/
Matrix porosity, θ, (–)	0.005	/Lindgren et al. 2001/
Pathlength, L_{tot}, (m)	60	Assumed
Groundwater velocity, υ, ($m\ y^{-1}$)	1.2	Calculated as L_{tot}/t_f
Depth of thin matrix layer, d_0 (m)	0.0001	Calculated for Pu
Depth of 1st matrix compartment, d_1 (m)	0.0005	Fitted so that the total depth of the matrix compartments matches the maximum diffusion depth in the FARF31 calculations of 2.0 m
Depth of 2nd matrix compartment, d_2 (m)	0.0025	
Depth of 3rd matrix compartment, d_3 (m)	0.0125	
Depth of 4th matrix compartment, d_4 (m)	0.0625	
Depth of 5th matrix compartment, d_5 (m)	0.3125	
Depth of 6th matrix compartment, d_6 (m)	1.6095	

9.4 Comparison of models

Figure 9-2 shows a comparison of the estimated geosphere flux from the BLA for AMBER and FARF31. The open symbols are FARF31and the lines are AMBER. The AMBER geosphere model was configured to use output from BLA NUCFLOW model as input. For the majority of radionuclide the output times for FARF31and AMBER are identical, however, as FARF31simulations are undertaken individually for each radionuclide some radionuclides have different output times.

Generally AMBER estimates the maximum fluxes of non-sorbing (e.g. Mo-93) and slightly sorbing radionuclides (e.g. Ni-59) well, although AMBER tends to slightly underestimate the tails of the breakthrough curves for slightly sorbing radionuclides. The plots for strongly sorbing radionuclides such as Tc-99 and Pu-239 show some differences which are particularly apparent for the breakthrough when the contributions from dispersion are important.

A summary is given below in Table 9-2 of the comparison of the AMBER and FARF31 model results. The results for release from the BLA are chosen to correspond to the figure above. In each cell the first number is the maximum flux (Bq/y) and the second number in parentheses is the time of maximum flux (years).

It is considered that AMBER is capable of producing an acceptable agreement to FARF31 for the purposes of a post-closure safety assessment.

Table 9-2. Summary of comparisons of maximum radionuclide flux and time of maximum for AMBER and FARF31 geosphere models.

Radionuclide	Maximum radionuclide flux, Bq y^{-1} (time of max, y)	
	AMBER	FARF31
C-14in	1.7E+07 (1.3E+03)	1.8E+07 (1.3E+03)
Cl-36	5.5E+04 (1.2E+03)	6.7E+04 (1.2E+03)
Ni-59	1.1E+07 (1.8E+03)	1.0E+07 (1.7E+03)
Ni-63	9.9E+07 (1.8E+02)	8.0E+07 (1.8E+02)
Sr-90	2.6E+07 (5.8E+01)	2.5E+07 (5.8E+01)
Mo-93	1.2E+05 (1.2E+03)	1.3E+05 (1.2E+03)
Tc-99	4.1E+05 (6.8E+03)	3.5E+05 (1.1E+04)
Cs-135	3.4E+03 (2.5E+03)	2.9E+03 (2.8E+03)
Pu-239	9.1E+02 (2.5E+04)	6.2E+02 (2.5E+04)

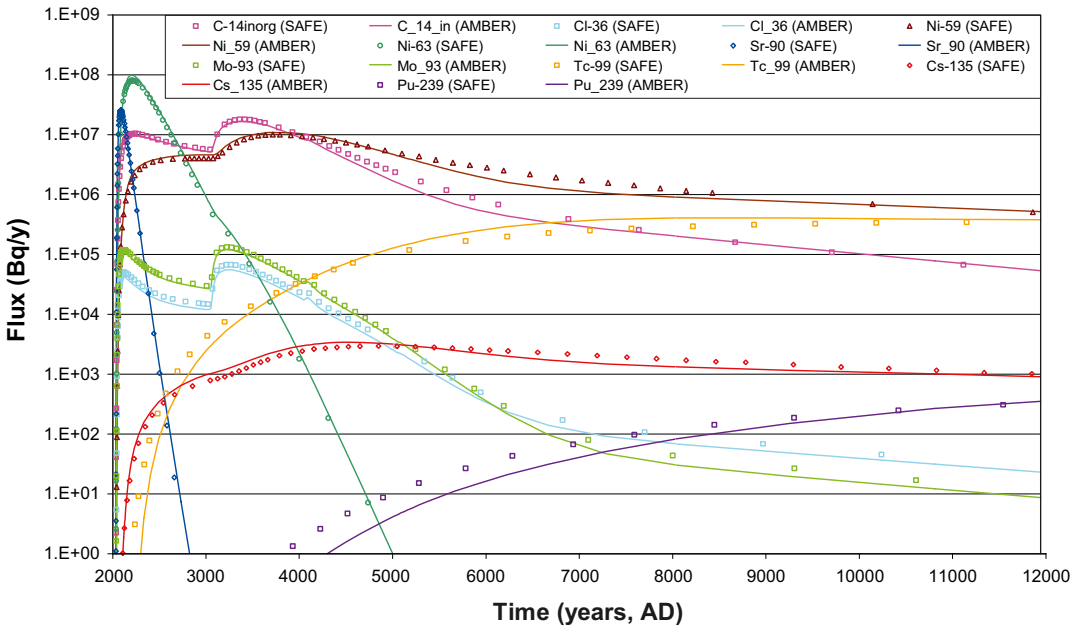

Figure 9-2. *Results from AMBER geosphere model (release from NUCFLOW BLA model).*

10 Reasonable biosphere development model

10.1 Model discretisation

The biosphere models used in Project SAFE are described by /Karlsson et al. 2001/, and provide the basis for the AMBER biosphere calculations. The basic models are described in detail in Appendix A. The scenario assessing release during reasonable biosphere development is considered here.

As in biosphere codes used in Project SAFE, AMBER applies a first-order differential equation to numerically solve each transfer expression between compartments and uses transfer coefficients, or rate constants, to model the annual migration and accumulation of radionuclides.

For the reasonable biosphere development case, the various defined stages of biosphere development comprise: release into today's biosphere conditions (prevailing until 5,000 AD, with a reduction in receptor volume at 4,000 AD); release to a lake (prevailing until 8,000 AD); and release to agricultural land (prevailing until 12,000 AD). Figure 10-1 below illustrates the progressive biosphere development.

10.1.1 Configuration of a reasonable biosphere development model in AMBER

Of particular note in the reasonable biosphere development is the need to represent the evolution from coastal receptor to a lake and then to agricultural land. As part of the representation of evolution, contamination resulting from activity that was discharged during earlier periods is conserved in the models for the later periods. This is done conveniently in AMBER by having continuity of the relevant compartments, as indicated below.

- Model Area (Marine) Upper Sediment → Agricultural Land Deep Soil.
- Lake Sediment → Agricultural Land Top Soil.
- Model Area (Marine) Deep Sediment → Agricultural Land Saturated Solid.

In order to ensure that the biosphere models are configured correctly in AMBER it is necessary to encode all the transfers in the models and then ensure that the correct sub-set of transfers only operate within the appropriate time period. This was achieved by using time-dependent parameters as "on-off" switches (which multiplied transfer rates by 0 to turn them off and by 1 to turn them on).

10.2 Mathematical representation

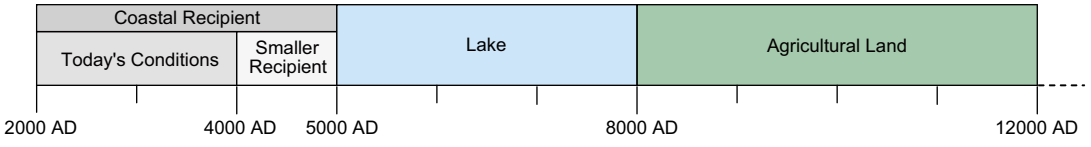

Figure 10-1. *Timeline of stages in Reasonable Biosphere Development.*

The changes in the biosphere conditions affect the exposure pathways through which radionuclides are taken-up by human and non-human biota. Information on the biosphere configuration in Project SAFE was taken from /Karlsson et al. 2001/. A fuller description of the mathematical relationships and data used is given in Appendix A.

Two parameters required further consideration before they could be represented in AMBER. They are the calculation of radionuclide concentrations in:

- irrigated root crops (edible part underground), and
- irrigated root vegetables (above-ground parts eaten).

The concentration of radionuclides in irrigated root crops, U_i [Bq kg^{-1}], is given as /Karlsson et al. 2001/:

$$U_i = C_s \cdot RUF_R + \sum_0^{Nr_{IRR}} I \cdot TL \cdot C_w \qquad \text{Equation 10-1}$$

where

C_s = Concentration of radionuclides in soil [Bq kg^{-1}dw] from the dispersion model,
RUF_R = Root uptake factors for root crops (soil to plant transfer factors) [(Bq kg^{-1} ww)/(Bq kg^{-1} dw)],
Nr_{IRR} = Number of irrigation occasions [y^{-1}],
I = Remaining water on the vegetation after each irrigation occasion [m^3 m^{-2}],
TL = Translocation from plant surface to edible parts of plant, [(Bq kg^{-1}ww)/(Bq m^{-2})],
C_w = Concentration of radionuclides in irrigation water [Bq m^{-3}], from the dispersion model.

This was implemented in AMBER as follows:

$$U_i = C_s \cdot RUF_R + Nr_{IRR2} \cdot I \cdot TL \cdot C_w \qquad \text{Equation 10-2}$$

where

Nr_{IRR2} = Annual number of irrigation events [–].

The concentration of radionuclides in irrigated root vegetables, U_v [Bq kg^{-1}], is given as /Karlsson et al. 2001/:

$$U_v = C_s \cdot RUF_v + \frac{C_w}{Y_v} \cdot \frac{I}{t_{tot}} \cdot \sum_{Nr_{IRR}} \int_0^{t_n} e^{-\tau \cdot t_n} dt \qquad \text{Equation 10-3}$$

where

C_s = Concentration of radionuclides in soil [Bq kg^{-1}dw], from the dispersion model,
RUF_v = Root uptake factor for vegetables (soil to plant transfer factor) [(Bq kg^{-1} ww)/Bq kg^{-1} dw)],
C_w = Concentration of radionuclides in irrigation water [Bq m^{-3}], from dispersion model,
Y_v = Yield of vegetables [kg m^{-2}·y^{-1}],
I = Remaining water on the vegetation after each irrigation occasion [m^3 m^{-2}],
t_{tot} = Irrigation period, fraction of year [–],
Nr_{IRR} = Number of irrigation occasions per year [y^{-1}],
t_n = Time between last irrigation occasion and harvest [days],
τ = ln(2)/$T_{½w}$ where $T_{½w}$ = weathering half-life [day].

This was implemented in AMBER as follows:

$$U_v = C_s \cdot RUF_v + Nr_{IRR} \frac{C_w}{Y_v} \cdot \frac{I}{t_{tot}} \cdot \frac{1}{\tau}\left(1 - e^{-\tau t_n}\right) \qquad \text{Equation 10-4}$$

10.3 Model parameterisation

The Project SAFE biosphere calculations were undertaken probabilistically using sampled parameters, some of which were correlated. Parameter values were taken from those reported in /Karlsson et al. 2001/. Correlated datasets were produced external to AMBER using the @risk software /http://www.palisade.com/. Simulations of 1,000 Monte Carlo samples were performed, a similar number to the runs in Project SAFE.

10.4 Comparison of models

Figure 10-2 below shows a comparison of the estimated annual individual dose for release from the BMA for reasonable biosphere development for the AMBER and Project SAFE models[6]. The open symbols are Project SAFE and the lines are AMBER. The AMBER model was configured to use output from BMA NUCFLOW model as input.

A summary is given below in Table 10-1 of the comparison of the AMBER and Project SAFE reasonable biosphere development model results. The results for release from the BMA are chosen to correspond to the figure above. In each cell the first number is the maximum average annual individual dose (Sv/y^{-1}) and the second number in parentheses is the time of maximum average annual individual dose (years).

Of particular note here is the relative scarcity of output times for the biosphere models compared to the near-field and geosphere. A reduced number of output times are often used when undertaking probabilistic runs in order to produce output files of a manageable size. The AMBER runs were undertaken using similar output times in order to provide a meaningful comparison.

Table 10-1. Summary of comparisons for AMBER and Project SAFE Reasonable Biosphere Development models for release from the BMA for selected radionuclides.

Maximum average annual individual dose ($Sv\ y^{-1}$)	AMBER	Project SAFE
Inorganic C-14	1.7E–08 (6.0E+03)	1.3E–08 (3.0E+03)
Organic C-14	5.6E–07 (3.0E+03)	5.2E–07 (3.0E+03)
Cl-36	1.9E–09 (7.2E+03)	3.3E–08 (6.0E+03)
Ni-59	2.9E–08 (6.0E+03)	2.5E–08 (6.0E+03)
Se-79	3.6E–07 (6.0E+03)	1.1E–07 (6.0E+03)
Mo-93	3.7E–08 (8.8E+03)	3.1E–09 (8.8E+03)
Tc-99	6.3E–10 (6.0E+03)	1.7E–09 (6.0E+03)
Ag-108m	5.6E–10 (6.0E+03)	6.3E–11 (3.1E+03)
I-129	1.3E–08 (1.2E+04)	1.2E–08 (1.2E+04)
Cs-135	2.8E–08 (6.0E+03)	1.7E–08 (6.0E+03)

[6] The comparison shown is for the arithmetic mean of the values resulting from the 1,000 realisations. Although upper and lower confidence limits were derived for the AMBER simulation, no confidence limits from Project SAFE were available for comparisons.

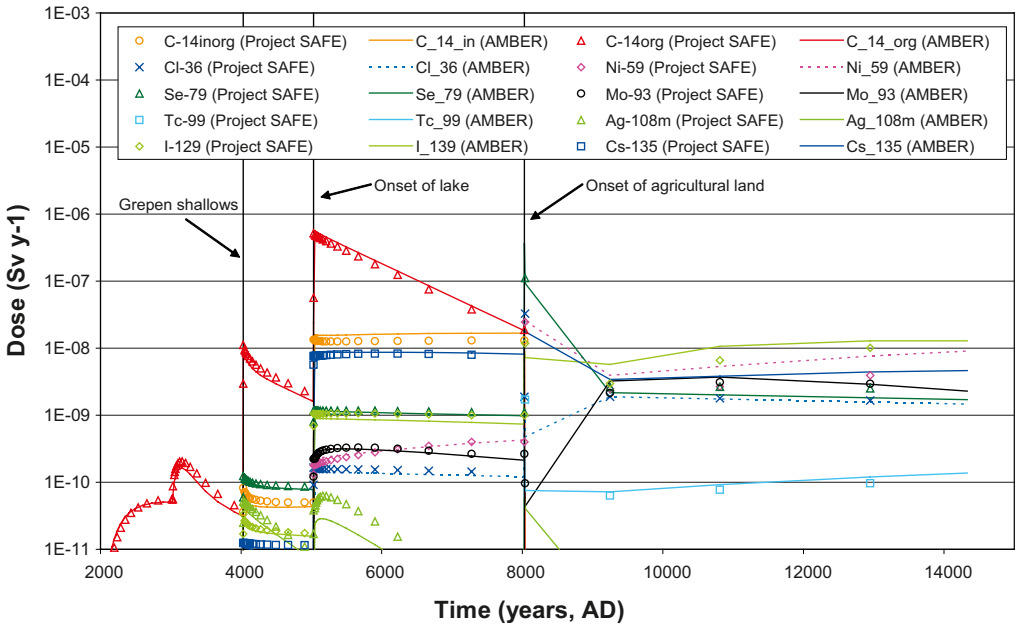

Figure 10-2. *Comparison of simulations for RBD (release from NUCFLOW BMA model).*

In Figure 10-2 the following step changes in results can be identified.

- By 4,000 AD as land uplift continues the coastal area of the Baltic in which the radionuclides discharge (the "Grepen") is considered to be shallower with reduced rates of turnover which, at the step-change in the model, results in a sudden increase in estimated doses.
- At 5,000 AD in response to continued land uplift the Baltic retreats further and the radionuclides are considered to discharge into lake. The lake has a lower volume and rate of turnover than the Baltic environment and associated with it is the use of the lake water for irrigation of foodstuffs. Again a sudden increase in doses is associated with the reduction in dilution and also the introduction of additional exposure pathways.
- At 8,000 AD groundwater is assumed to discharge directly to land which is used for agricultural purposes. An important point to note here is that, after the step-change in the model, sediments that were previously contaminated with radionuclides during the coastal and lake periods form part of the soils and subsurface materials. A consequence of this is that for many radionuclides the peak doses are estimated for the agricultural land period at the onset of agricultural conditions, being associated with the sudden release of radionuclides that have accumulated during the coastal and lake periods[7].

In addition there is a change in the near-field flowfields at 3,000 AD which is not marked on the figure but is discernible as an increase in estimated doses (from organic C-14) at this time.

Generally it can be seen that the model configured in AMBER is well able to represent the results of the original Project SAFE calculations. However, some notable differences exist which are discussed below.

[7] As noted previously the output times selected for the biosphere are dispersed relatively sparsely through the assessment period, particularly from 6,000 years onwards. During the initial stages of the land period output is given at 6,000, 6,010 and c 7,210 years. More detailed studies have shown that the impact of the retained radionuclides is short-lived and in fact quicker than the impression that it is given in Figure 10-2.

The times at which maximum doses are estimated generally compare well between the two sets of model results with the exception of inorganic C-14, Cl-36 and Ag-108m.

- In Project SAFE the maximum dose from inorganic C-14 is estimated at 6,000 years (end of the Lake period and onset of Agricultural land), whereas in AMBER it is estimated at 3,000 years (at the onset of the Lake period). The dose rates are nearly horizontal for both models between these times, the doses in Project SAFE increase slightly whilst those estimate from AMBER decrease slightly.
- In Project SAFE the maximum dose from Cl-36 is estimated at 6,000 years (end of the Lake period and onset of Agricultural land), whereas in AMBER it is estimated at 7,200 years (during the Agricultural land period).
- In Project SAFE the maximum dose from Ag-108m is estimated at 3,100 years (at the beginning of the Lake period), whereas in AMBER it is estimated at 6,000 years (end of the Lake period and onset of Agricultural land).

It is believed that the main reasons for this behaviour may be associated with the lake model implemented in AMBER. A review has been undertaken of the biosphere models developed for SR 97 (on which the biosphere used in Project SAFE were based) as part of another code development exercise /Jones et al. 2004/. This review highlighted some areas, particularly associated with the lake model (and associated irrigation model) in which discrepancies exist between the approach reported and that actually adopted.

Some differences are also noted for the doses estimated during the coastal and agricultural periods. It is possible that the causes of the differences in the agricultural land period may be due to discrepancies in the lake model, as noted in other studies /e.g. Jones et al. 2004/. These may result in differences in radionuclides retained in sediments that are subsequently used in the agricultural land model. However, this could not be the cause of the differences noted for the preceding coastal period model.

Furthermore, the comparison of the maximum average annual individual doses estimated in Project SAFE and AMBER suggest that there may be other differences present. The biosphere models used in Project SAFE are reported in /Karlsson et al. 2001/ and are based on those developed previously for SR 97 /Bergström et al. 1999/.

The following changes to the SR 97 models are stated to have been made as part of Project SAFE /Karlsson et al. 2001/.

1. The models were modified to enable the use of time dependent source terms instead of the unit releases.
2. The coastal model was modified in order to make it more site-specific and also to represent the impacts of land uplift on it.
3. A general review of the data was undertaken.

A general comparison of the biosphere models reported in /Bergström et al. 1999, Karlsson et al. 2001, Jones et al. 2004/ indicates there are differences between the modelling approaches and also in the data used. As noted previously the review of /Jones et al. 2004/ highlighted some discrepancies in the original documentation of SR 97 /Bergström et al. 1999/. Some of these discrepancies had been addressed in the data review carried out as part of the biosphere development for Project SAFE. Some values remained unchanged from /Bergström et al. 1999/ and other values differed.

However, it was not possible to determine if the biosphere models reported in /Jones et al. 2004/ were the definitive set because the mathematical approach differed from that reported in /Karlsson et al. 2001/ in some areas. Also the study in /Jones et al. 2004/ was by nature designed to be generic whereas the assessment for Project SAFE was obviously site specific. Therefore some parameters such as volumes, depths, and flowrates may vary for good reasons.

Notwithstanding the points above, it is considered that AMBER is well able to represent the reasonable biosphere development model.

11 Today's Biosphere model

11.1 Model description

In the Today's Biosphere model the biospheric conditions remain unchanged throughout the assessment period. The model used for all times is the same as that for the first 2,000 years in the reasonable biosphere development (Section 10), which is a coastal model describing the present conditions in Öregrundsgrepen. The exposure pathways considered are thus consumption of fish as well as consumption of milk and meat from cattle grazing at the shore.

11.2 Comparison of models

Figure 11-1 below shows a comparison of the estimated annual individual dose for release from the BLA to Today's Biosphere for the AMBER and Project SAFE models[8]. The open symbols are Project SAFE and the lines are AMBER. The AMBER model was configured to use output from BLA NUCFLOW model as input.

A summary is given below in Table 11-1 of the comparison of the AMBER and Project SAFE Today's Biosphere model results. The results for release from the BLA are chosen to correspond to the figure above. In each cell the first number is the maximum average annual individual dose (Sv y^{-1}) and the second number in parentheses is the time of maximum average annual individual dose (years)[9].

Generally the models agree well although the maximum average individual doses estimated for some radionuclides do show some differences, particularly in the case of inorganic C-14.

Given the similarity of Today's Biosphere to the coastal model, the source of such differences is considered to be the same as those identified previously for the reasonable biosphere development model.

Table 11-1. Summary of comparisons for AMBER and Project SAFE Today's Biosphere models for release from the BLA for selected radionuclides.

	Maximum average annual individual dose (Sv y^{-1})	
	AMBER	Project SAFE
Inorganic C-14	3.6E–11 (0.5)	3.9E–11 (0.5)
Co-60	4.5E–10 (0.5)	4.6E–11 (0.5)
Ni-63	2.0E–10 (0.5)	2.0E–10 (0.5)
Sr-90	3.1E–10 (0.5)	3.0E–10 (0.5)
Cs-137	1.1E–08 (0.5)	1.1E–08 (0.5)
Eu-154	1.6E–10 (0.5)	1.7E–10 (0.5)
Pu-238	2.6E–11 (0.5)	2.6E–11 (0.5)
Am-241	5.0E–11 (0.5)	5.0E–11 (0.5)

[8] The comparison shown is for the arithmetic mean of the values resulting from the 1,000 realisations. Although upper and lower confidence limits were derived for the AMBER simulation, no confidence limits from Project SAFE were available for comparisons.

[9] The results from the Project SAFE Today's Biosphere model show a non-zero estimated dose at time zero, whereas the AMBER models shows a zero value until the first output time, 0.5 years, which has been chosen as the comparison time for this reason.

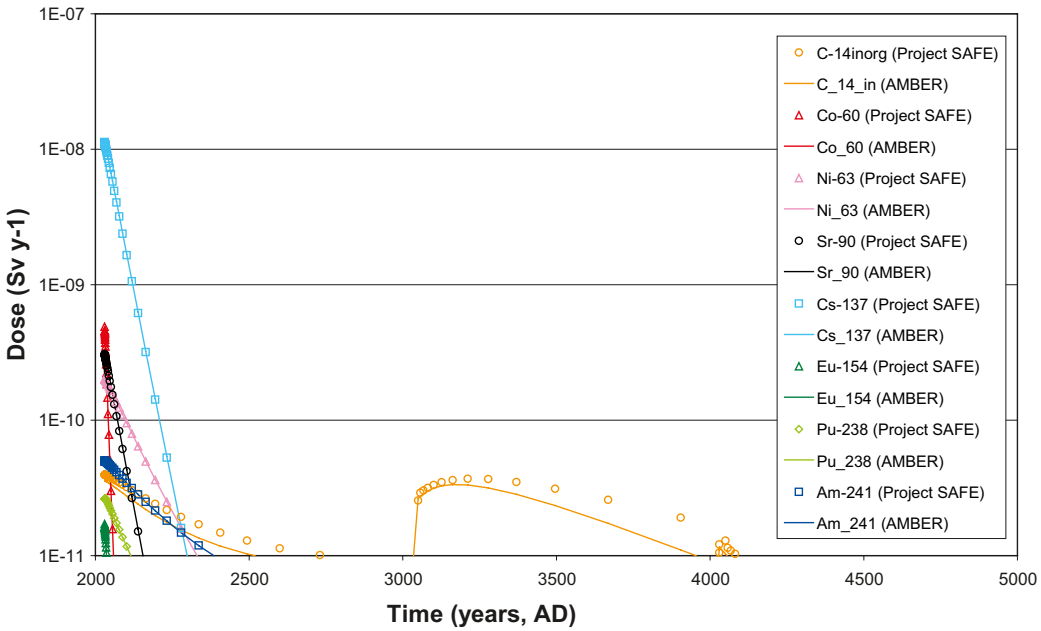

Figure 11-1. *Comparison of results for release from the BLA to Today's Biosphere for selected radionuclides.*

12 Release to a mire

/Jones et al. 2004/ describe and document calculations undertaken on the various biosphere models used in SKB's SR 97 assessment. These models included a mire (peat bog) biosphere. A comparison was made of the performance of AMBER against TENSIT, the simulation tool used in /Jones et al. 2004/.

Therefore, the main purpose of the exercise is to demonstrate the ability of AMBER to replicate the results of SKB biosphere analyses.

12.1 Model description

An AMBER model was configured following the description of the well biosphere model documented in /Jones et al. 2004/. A screenshot of the AMBER model is shown in Figure 12-1. The model consists of three compartments to represent the soluble fraction, the solid fraction and a sink for losses from the system.

The transfer of radionuclides into the mire is modelled, as is movement within the system due to outflow from the mire, sorption and desorption.

12.2 Mathematical representation

The transfer of radionuclides from the mire out of the system, $\lambda_{outflow}$ (y^{-1}), is represented as follows:

$$\lambda_{outflow} = 1 - \frac{R}{\varepsilon_p \cdot D_p} \qquad \text{Equation 12-1}$$

where

R is the runoff [$m^3/(m^2\ y^{-1})$],

ε_p is the porosity of the mire [–],

D_p is the depth of the mire [m].

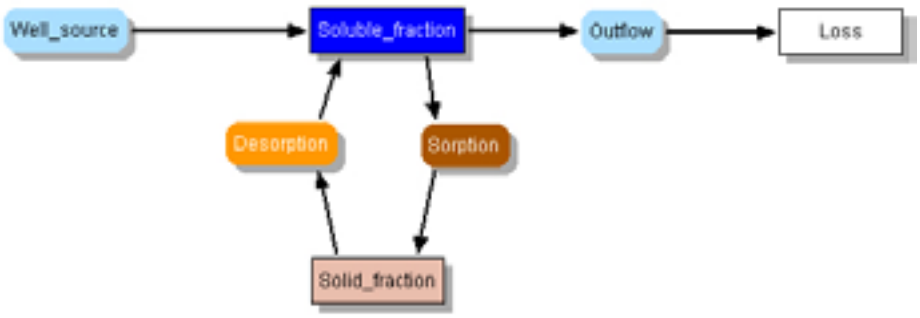

Figure 12-1. *AMBER mire model.*

The transfer of radionuclides from the soluble fraction to the solid fraction (by sorption), $\lambda_{sorption}$ (y^{-1}), is represented as follows:

$$\lambda_{sorption} = \frac{K_d \cdot \ln(2)}{T_k} \frac{\rho_p}{\varepsilon_p}$$ Equation 12-2

where

K_d is the radionuclide-specific distribution coefficient [m^3 kg^{-1}],

ρ_p is the peat density [kg m^{-3}],

T_k is the reaction half time [y].

The transfer of radionuclides from the solid fraction to the soluble fraction (by desorption), $\lambda_{desorption}$ (y^{-1}), is represented as follows:

$$\lambda_{desorption} = \frac{\ln(2)}{T_k}$$ Equation 12-3

12.3 Model parameterisation

The AMBER model was parameterised to undertake a deterministic simulation. Given the limited scope probabilistic simulations were not undertaken. The data used are summarised in /Jones et al. 2004/.

12.4 Comparison of models

Table 12-1 below compares the estimated distribution of radionuclides within the biosphere system at 10,000 years following a unit input for a deterministic simulation. Differences in results are highlighted in bold. It can be seen that the agreement between AMBER and TENSIT is good.

Table 12-1. Comparison of deterministic results from AMBER and TENSIT mire models.

Distribution of radionuclides (%)	Cl-36	Mo-93	Np-237	I-129	Ni-59	Cs-135	Pu-239
Tensit							
Water	0.019	0.043	0.019	0.019	0.02	0.019	0.021
Organic	0.021	0.144	2.087	0.063	2.17**8**	0.626	4.7**26**
Out	99.960	99.813	97.895	99.919	97.802	99.355	95.2**33**
AMBER							
Water	0.019	0.043	0.019	0.019	0.020	0.019	0.021
Organic	0.021	0.143	2.087	0.063	2.17**7**	0.626	4.7**38**
Out	99.960	99.814	97.895	99.919	97.804	99.355	95.2**40**

13 Release to a well

/Jones et al. 2004/ describe and document calculations undertaken on the various biosphere models used in SKB's SR 97 assessment. These models included a well biosphere. A comparison was made of the performance of AMBER against TENSIT, the simulation tool used in /Jones et al. 2004/.

It should be noted that this differed from that in Project SAFE slightly in terms of the description of irrigation and some of the parameters used to calculate exposures. However, the main purpose of the exercise is to demonstrate the ability of AMBER to replicate the results of SKB biosphere analyses.

13.1 Model description

An AMBER model was configured following the description of the well biosphere model documented in /Jones et al. 2004/. A screenshot of the AMBER model is shown in Figure 13-1. The model consists of four compartments to represent: the well, top soil, deep soil and a sink for losses from the system.

The transfer of radionuclides from the well via irrigation is modelled, as is movement within the system due to outflow from the well, soil erosion, soil removal, leaching and biotransport.

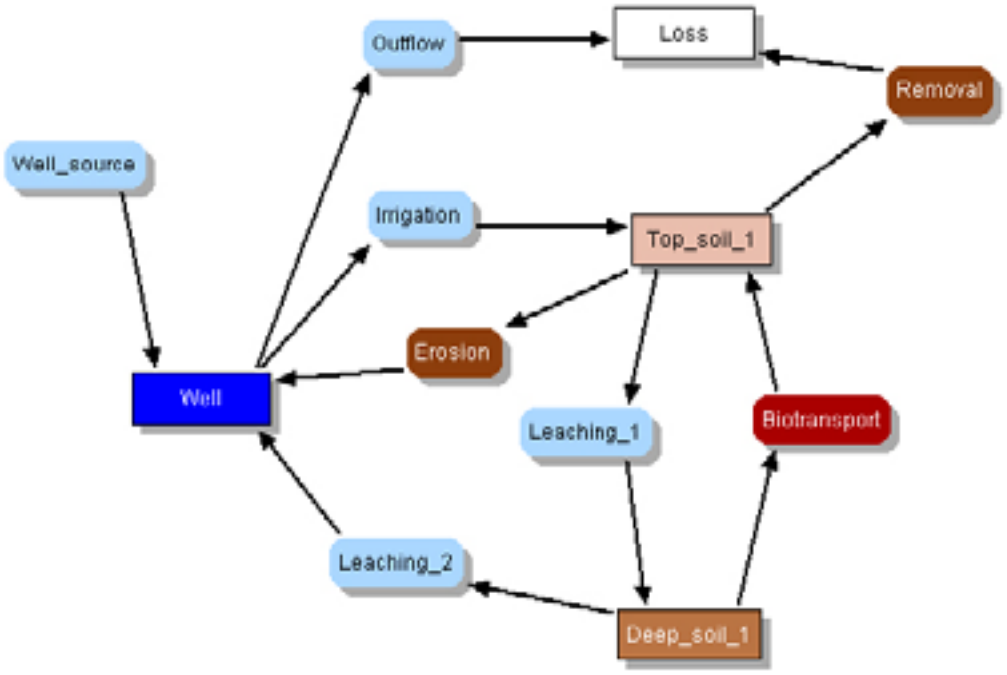

Figure 13-1. *AMBER well model.*

13.2 Mathematical representation

The transfer of radionuclides from the well to land during irrigation, $\lambda_{irrigation}$ (y^{-1}), is represented as follows:

$$\lambda_{irrigation} = \frac{I}{V_{mix}}$$ Equation 13-1

where

I is the annual volume of irrigation water [$m^3\ y^{-1}$], which is calculated from

$$I = Irr_{volume} \cdot Area_{irrigation}$$ Equation 13-2

Irr_{volume} is the volume of irrigation water applied annually per unit area [$m^3/(m^2\ y)$],

$Area_{irrigation}$ is the area irrigated [m^2],

V_{mix} is the annual mixing volume [m^3], taken to be

$$V_{mix} = C_{well} \cdot 1[\mathrm{y}]$$ Equation 13-3

C_{well} is the water capacity of the well [$m^3\ y^{-1}$].

The transfer of radionuclides from the well out of the system, $\lambda_{outflow}$ (y^{-1}), is represented as follows:

$$\lambda_{outflow} = 1 - \frac{I}{V_{mix}}$$ Equation 13-4

The transfer of radionuclides from the top soil back to the irrigation source via erosion, $\lambda_{erosion}$ (y^{-1}), is represented as follows:

$$\lambda_{erosion} = \frac{Eros}{h_s}$$ Equation 13-5

where

$Eros$ is the soil erosion rate [$m\ y^{-1}$],

h_s is the depth of top soil [m].

The removal of radionuclides from the top soil, for example via weeding, $\lambda_{removal}$ (y^{-1}), is represented as follows:

$$\lambda_{removal} = \frac{Rem}{h_s(1-\varepsilon)\cdot\rho_p}$$ Equation 13-6

where

Rem is the removal rate of soil [$kg/(m^2\ y)$],

ε is the porosity of the top soil [–],

ρ_p is the soil particle density [$kg\ m^{-3}$].

The transfer of radionuclides from top soil to deep soil, (y^{-1}), is represented as follows.

$$\lambda_{leaching\_1} = \frac{R}{\varepsilon \cdot h_s} Ret + \frac{BioT}{h_s(1-\varepsilon)\cdot\rho_p}$$ Equation 13-7

where
R is the runoff [$m^3/(m^2\ y^{-1})$],
$BioT$ is the rate of biotransport due to bioturbation [$kg/(m^2\ y)$],
Ret is the retardation of radionuclides on soil [–], given by

$$Ret = \frac{1}{1 + K_d \cdot \rho_p \frac{1-\varepsilon}{\varepsilon}}$$ Equation 13-8

K_d is the radionuclide-specific distribution coefficient [$m^3\ kg^{-1}$].

The transfer of radionuclides from deep soil to top soil, $\lambda_{biotransport}$ (y^{-1}), is represented as follows:

$$\lambda_{biotransport} = \frac{BioT}{h_{ds}(1-\varepsilon_{ds}) \cdot \rho_p}$$ Equation 13-9

where
h_{ds} is the depth of deep soil [m],
ε_{ds} is the porosity of deep soil [–].

The transfer of radionuclides from deep soil back to the irrigation source, $\lambda_{leaching\_2}$ (y^{-1}), is represented as follows:

$$\lambda_{leaching\_2} = \frac{R}{\varepsilon_{ds} \cdot h_{ds}} Ret$$ Equation 13-10

where

$$Ret = \frac{1}{1 + K_d \cdot \rho_p \frac{1-\varepsilon_{ds}}{\varepsilon_{ds}}}$$ Equation 13-11

13.3 Model parameterisation

The AMBER model was parameterised to undertake a deterministic simulation. Given the limited scope probabilistic simulations were not undertaken. The data used are summarised in /Jones et al. 2004/.

13.4 Comparison of models

Table 13-1 below compares the estimated distribution of radionuclides within the biosphere system at 10,000 years following a unit input for a deterministic simulation. Differences in results are highlighted in bold. It can be seen that the agreement between AMBER and TENSIT is good.

Table 13-1. Comparison of deterministic results from AMBER and TENSIT well models.

Distribution of radionuclides (%)							
	Cl-36	**Mo-93**	**Np-237**	**I-129**	**Ni-59**	**Cs-135**	**Pu-239**
Tensit							
Well water	0.011	0.025	0.011	0.011	0.011	0.011	0.012
Top soil	0.002	0.303	0.146	0.429	0.669	0.991	1.634
Deep soil	0.007	1.096	0.569	1.658	2.539	3.69**3**	5.793
Out	99.98	98.576	99.273	97.902	96.78**1**	95.30**6**	92.561
AMBER							
Well water	0.011	0.025	0.011	0.011	0.011	0.011	0.012
Top soil	0.002	0.303	0.146	0.429	0.669	0.991	1.634
Deep soil	0.007	1.096	0.569	1.658	2.539	3.69**4**	5.793
Out	99.980	98.576	99.273	97.902	96.78**0**	95.30**4**	92.561

14 Summary

This report documents an exercise in which AMBER has been used to represent Project SAFE, a safety assessment undertaken on SFR 1.

AMBER has been used to undertake assessment calculations on all of the disposal system, including all disposal tunnels and the Silo, the geosphere and several biosphere modules.

The conceptual models employed in Project SAFE have required the consideration of time-dependency in certain aspects of the near-field and biosphere. The geosphere model developed was required to represent radionuclide transport within a fractured granite geosphere. In addition the biosphere models used several datasets which were sampled in order that probabilistic calculations could be undertaken.

In undertaking the comparison of AMBER with the various codes and calculation tools used in Project SAFE it was necessary to undertake a detailed analysis of the modelling approach previously adopted, particular focus was given to the near-field. As a result some discrepancies in the implementation of the models and documentation were noted.

AMBER has demonstrated that it is fully capable of representing the features of the SFR 1 disposal system in a safety assessment.

15 References

Bergström U, Nordlinder S, Aggeryd I, 1999. Models for dose assessments: Modules for various biosphere types. SKB TR-99-14, Svensk Kärnbränslehantering AB.

Cronstrand P, 2005. Assessment of uncertainty intervals for sorption coefficients. SFR 1 uppföljning av SAFE. SKB R-05-75, Svensk Kärnbränslehantering AB.

Enviros, Quintessa, 2006. AMBER 5 Reference Guide, Version 1.0, September 2006, Enviros, Culham.

Holmén J G, Stigsson M, 2001. Modelling of future hydrogeological conditions at SFR. SKB R-01-02, Svensk Kärnbränslehantering AB.

IAEA, 2004. Safety Assessment Methodologies for Near Surface Disposal Facilities: Results of a co-ordinated research project. Volume 2 Test cases. International Atomic Energy Agency, Vienna.

Jones J, Vahlund F, Kautsky U, 2004. Tensit – a novel probabilistic simulation tool for safety assessments. Tests and verifications using biosphere models. SKB TR-04-07, Svensk Kärnbränslehantering AB.

Karlsson S, Bergström U, Meili M, 2001. Models for dose assessments. Models adapted to the SFR-area, Sweden. SKB TR-01-04, Svensk Kärnbränslehantering AB.

Kautsky U, 2001. The biosphere today and tomorrow in the SFR area. SKB R-01-27, Svensk Kärnbränslehantering AB.

Lindgren M, Pettersson M, Karlsson S, Moreno L, 2001. Project SAFE. Radionuclide release and dose from the SFR repository. SKB R-01-18, Svensk Kärnbränslehantering AB.

Maul P, Robinson P C, 2002. Exploration of Important Issues for the Safety of SFR 1 using Performance Assessment Calculations, SKI report 2002:62.

Maul P, Robinson P, Avila R, Broed R, Pereira A, 2003. Xu S., AMBER and Ecolego Intercomparisons – using Calculations from SR 97, SKI report 2003:28, SSI report 2003:11.

Moreno L, Skagius K, Södergren S, Wiborgh M, 2001. Project Safe. Gas related processes in SFR. SKB R-01-11, Svensk Kärnbränslehantering AB.

Norman S, Kjellbert N, 1990. FARF31 – A far field radionuclide migration code for use with the PROPER package. SKB TR 90-01, Svensk Kärnbränslehantering AB.

Påsse T, 1997. A mathematical model of past, present and future shore level displacement in Fennoscandia. SKB TR 97-28, Svensk Kärnbränslehantering AB.

Robinson P C, Penfold J S S, Little R H, Walke R C, 2004. AMBER 4.6 Verification Summary. QRS-1059C-1. Version 1. Quintessa, Henley on Thames.

Robinson P C, 2008. AMBER White Paper: Modelling Rock Matrix Diffusion with AMBER Guidance Note. Quintessa, Henley on Thames.

SKB, 2001a. SFR 1 Safety Analyses Report. Svensk Kärnbränslehantering AB.

SKB, 2001b. Project SAFE: Compilation of data for radionuclide transport analysis. SKB R-01-14, Svensk Kärnbränslehantering AB.

SKI, SSI, 2004. SSI and SKI's Review of SKB's Updated Final Safety Report for SFR 1. Review Report. SKI Report 2004:47 (SSI Report 2004:06).

Appendix A

Reasonable biosphere development model

The information summarised here is taken from /Karlsson et al. 2001/.

Coastal and lake models

The compartments used to represent the coastal and lake modules of the reasonable biosphere development model are shown below. Arrows mark the direction of transfers and crosses mark the potential sources of radionuclides.

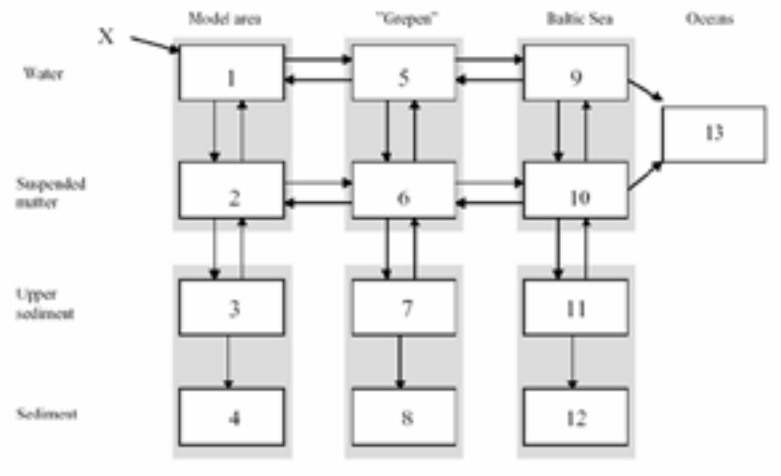

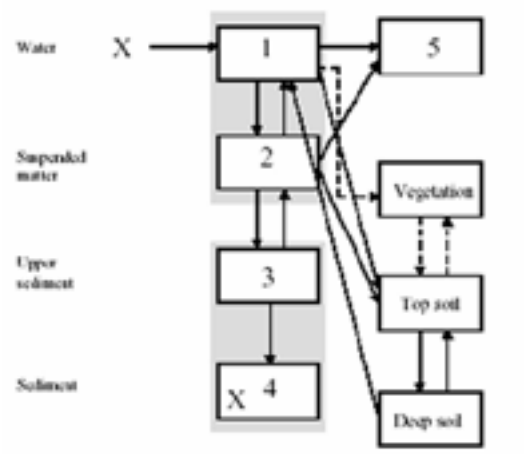

Turnover of water and suspended matter

The rate constant describing the transfer of water, and thereby radionuclides in solution, between the different water components of the system is obtained from the water retention time within each part. The radionuclides in the water or on suspended matter are assumed to move at the same rate as the carrying medium. The outflow of water (from the Model Area to Grepen, from Grepen to the Baltic Sea and from the Baltic Sea to the Oceans) is described as the fraction of water leaving a given region per unit of time, which is equivalent to the inverse of the water retention time, $\lambda_{turnover\_outflow}$ [y^{-1}]:

$$\lambda_{turnover\_outflow} = 1 / RETTIME_x \qquad \text{Equation A-1}$$

where

$RETTIME_x$ is the water retention time in the part from which water is transferred (Model Area, Grepen or Baltic Sea) [y].

The water inflow, $\lambda_{turnover\_inflow}$ [y^{-1}], to the Model Area from Grepen is related to the volume ratio of the two areas as follows:

$$\lambda_{turnover\_inflow} = \frac{A_M \cdot D_M}{A_G \cdot D_G} \cdot \frac{1}{RETTIME_M} \qquad \text{Equation A-2}$$

where

A_M = Area of Model Area [m^2],

A_G = Area of Grepen [m^2],

D_M = Mean water depth in the Model Area [m],

D_G = Mean water depth in Grepen [m],

$RETTIME_M$ = Water retention time in the Model Area [y].

The water inflow to Grepen from the Baltic Sea is obtained from the same expression but the values for the Model Area are replaced by those for Grepen and the values for Grepen by those for the Baltic.

The suspended matter follows the water and therefore the same transfer coefficients are used. Particulate matter as a whole may have a longer turnover time because of settling and resuspension, which is accounted for by the exchange of material between suspended and surficial sediments.

Interaction of radionuclides between water and particles

Radionuclides are assumed to be released in soluble form into the water in the Model Area. The sorption-desorption transfer of radionuclides between the water and the suspended matter (in the Model Area as well as in Grepen and the Baltic Sea) is assumed to reach an equilibrium, but not instantaneously. Therefore, the transfer from water to suspended matter is described by a rate of sorption, $\lambda_{sorption}$ [y^{-1}], that is proportional to the particle concentration and the radionuclide distribution coefficient.

$$\lambda_{sorption} = \frac{\ln 2}{T_k} Susp \cdot K_d \ [y^{-1}] \qquad \text{Equation A-3}$$

The rate of desorption, $\lambda_{desorption}$ [y^{-1}], from suspended matter to water is given by:

$$\lambda_{desorption} = \frac{\ln 2}{T_k}$$ Equation A-4

where

T_k = Half-time to reach sorption equilibrium [y],

Susp = Suspended matter in media [kg m^{-3}],

K_d = Distribution coefficient, ratio of element concentrations in the solid and the dissolved phase [m^3 kg^{-1}].

Sedimentation and resuspension

A fraction of the suspended matter is assumed to reach the upper sediment through sedimentation (gross sedimentation). The sedimentation transfer rate, $\lambda_{sedimentation}$ [y^{-1}], is described by:

$$\lambda_{sedimentation} = \frac{V_{sink}}{D}$$ Equation A-5

where

V_{sink} is the particle settling velocity [m y^{-1}],

D is the mean water depth in media [m].

A fraction of the deposited material is assumed to be transferred back to the water phase by resuspension and the remaining part is assumed to accumulate on the bottom sediments. The sediment is, therefore, described by two compartments, one for the upper, biologically active, sediment and one for the deeper layers. The turnover of radionuclides in the upper sediment is described by using the maximum growth rate of this sediment layer and the depth of mixing by bioturbation. The fluxes are partitioned according to the fraction of accumulation bottoms obtained from wave-theory based models of the area. Thus, the transfer from the upper sediment back to the suspended matter, $\lambda_{resuspension}$ [y^{-1}] , is described by:

$$\lambda_{resuspension} = \frac{G_s}{D_s}(1 - Frac)$$ Equation A-6

and the transfer from the upper sediment to deeper sediment layers, λ_{burial} [y^{-1}], is calculated using:

$$\lambda_{burial} = \frac{G_s}{D_s} Frac \ [y^{-1}]$$ Equation A-7

where

G_S = Sediment growth rate [m y^{-1}],

D_S = Depth of upper sediment [m],

Frac = Fraction of accumulation bottoms in media.

The irrigation sub-model which is used in the Lake Model is shown below.

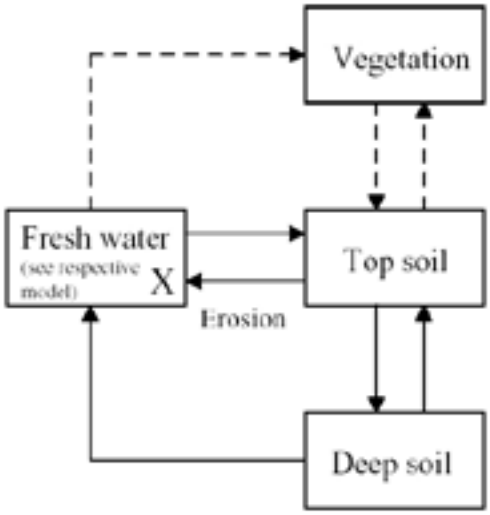

The rate constant describing the transfer of radionuclides from surface water to soil due to irrigation is obtained from the following expression:

$$\lambda_{irrigation} = \frac{V_{IRR} \cdot Nr_{IRR}}{V_W} A \, [y^{-1}] \qquad \text{Equation A-8}$$

where

V_{IRR} = Water amount used at each irrigation event [$m^3\,m^{-2}\,y^{-1}$],

Nr_{IRR} = Number of irrigation events per year [–],

V_W = Volume of water from which irrigation water is taken [m^3],

A = Area of irrigated soil [m^2].

It is assumed that the suspended matter follows the water and therefore the same transfer coefficient is used for the transfer of suspended matter to soil in the lake model.

After deposition on soils, nuclides migrate with varying rates due to their physical and chemical properties and soil conditions. In addition, processes like bioturbation and erosion cause a redistribution of the radionuclides. The transfer rate of radionuclides from the top soil to the deep soil compartments, $\lambda_{topsoil\_leaching}$ [y^{-1}], is described by:

$$\lambda_{topsoil\_leaching} = \frac{Runoff}{\varepsilon_t \cdot D_{ts}} \cdot R_f + \frac{BioT}{D_{ts}(1-\varepsilon_t)\rho_p} \qquad \text{Equation A-9}$$

where

$$R_f = \frac{1}{\left[1 + K_d \cdot \rho_p \cdot (1-\varepsilon_t)/\varepsilon_t\right]} \qquad \text{Equation A-10}$$

and

Runoff is the soil runoff [$m^3\,m^{-2}\,y^{-1}$],

ε_t = Porosity of soil in the top soil [$m^3\,m^{-3}$],

D_{ts} = Depth of top soil [m],

$BioT$ = Transport due to bioturbation [$kg\,m^{-2}y^{-1}$],

ρ_p = Density of soil particles [$kg\,m^{-3}$],

K_d = Distribution factor, concentration of the element on solids relative to dissolved [$m^3\,kg^{-1}$].

The bio-transport rate, $\lambda_{deepsoil\_transport}$ [y^{-1}], from deep soil to top soil is given by:

$$\lambda_{deepsoil\_transport} = \frac{BioT}{D_{ds}(1-\varepsilon_d)\rho_p}$$ Equation A-11

where

D_{ds} = Depth of deep soil layer [m], see below,

ε_d = Porosity of soil in the deep soil [$m^3\ m^{-3}$],

D_{ds} = $1-D_{ts.}$

where

D_{ts} = Depth of top soil [m].

Radionuclides in deep soil are assumed to leak back to the lake from which the irrigation water is taken. This is described by the same expression as above, but without bioturbation and with depths and porosities according to deep soil.

$$\lambda_{deepsoil\_leaching} = \frac{Runoff}{\varepsilon_t \cdot D_{ds}} \cdot R_f$$ Equation A-12

Agricultural land model

The compartments used to represent the agricultural land model of the reasonable biosphere development is shown below. Arrows mark the direction of transfers and crosses mark the potential sources of radionuclides.

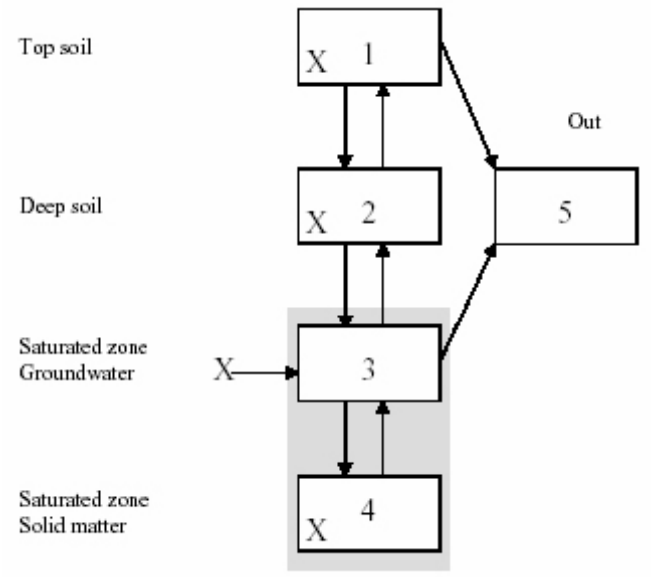

Transfers between solid and soluble fractions

The distribution of elements between dissolved and solid fractions in the saturated zone is described by one parameter (here called K_d) although it involves chemical, biological and physical processes. These are time-dependent processes and the soil sorption transfer rate, $\lambda_{soil\_sorption}$ [y^{-1}], is given by the expression:

$$\lambda_{soil\_sorption} = \frac{K_d \cdot \ln 2}{T_k} \cdot \frac{(1-\varepsilon_{sa}) \cdot \rho_{sa}}{\varepsilon_{sa}} \qquad \text{Equation A-13}$$

where

K_d = Distribution coefficient, concentration of the element on solids relative to dissolved [$m^3\ kg^{-1}$],

T_k = Half-time to reach sorption equilibrium [y],

ε_{sa} = Porosity in saturated zone [$m^3\ m^{-3}$],

ρ_{sa} = Density of soil particles [$kg\ m^{-3}$].

The soil desorption transfer rate, $\lambda_{desorption}$ [y^{-1}], is calculated as described previously by Equation A-4.

Transfer from saturated zone

The transfer rate describing the horizontal flow of dissolved radionuclides in groundwater outflow from the saturated zone, λ_{gw_loss} [y^{-1}], is based on water balance and becomes:

$$\lambda_{gw\_loss} = \frac{Runoff}{\varepsilon_{sa} \cdot D_{sa}} \qquad \text{Equation A-14}$$

Runoff [$m^3\ m^{-2}\ y^{-1}$],

ε_{sa} = Porosity in saturated zone [$m^3\ m^{-3}$],

D_{sa} = Depth of saturated zone [m].

Transfers between saturated zone and deep soil

The direction of water flow between saturated and unsaturated zones varies with time. Processes as diffusion and capillary rise cause an upward flow from the saturated to the unsaturated zone, during dry periods, while precipitation generates a flow in the opposite direction. The transfer rate from saturated to deep unsaturated soil, λ_{sat_deep} [y^{-1}], is:

$$\lambda_{sat\_deep} = \frac{F_{sa,\,ds}}{\varepsilon_{sa} \cdot D_{sa}} \qquad \text{Equation A-15}$$

where

$F_{sa,\,ds}$ = Upward flow [$m^3\ m^{-2}\ y^{-1}$],

ε_{sa} = Porosity in saturated zone [$m^3\ m^{-3}$],

D_{sa} = Depth of saturated zone [m].

The downward transfer of radionuclides from the deep soil to the saturated zone, λ_{deep_sat} [y^{-1}], is:

$$\lambda_{deep\_sat} = \frac{R + F_{ds,\,sa}}{\varepsilon_{ds} \cdot D_{ds}} R_f \qquad \text{Equation A-16}$$

where
$F_{ds,\,sa}$ = Downward flow [$m^3\,m^{-2}\,y^{-1}$],
R = Runoff [$m^3\,m^{-2}\,y^{-1}$],
ε_{ds} = Porosity in deep soil [$m^3\,m^{-3}$],
D_{ds} = Depth of deep soil [m],
R_f = Retention, (see below) [–],
D_{ds} = 1–$D_{ts.}$

where
D_{ts} = Depth of top soil [m].

Transfers between deep soil and top soil

The transfer rate from deep soil to top soil, λ_{deep_top} [y^{-1}], is:

$$\lambda_{deep\_top} = \frac{F_{ds,\,ts}}{\varepsilon_{ds} \cdot D_{ds}} R_f + \frac{BioT}{(1-\varepsilon_{ds}) \cdot \rho_p \cdot D_{ds}} \qquad \text{Equation A-17}$$

where
$F_{ds,\,ts}$ = Upward flow [$m^{-3}\,m^{-2}\,y^{-1}$],
ε_{ds} = Porosity of deep soil [$m^3\,m^{-3}$],
D_{ds} = Depth of deep soil [m], see above,
R_f = Retention, see above [–],
$BioT$ = Bioturbation, (transport of soil by earthworms) [$kg\,m^{-2}\,y^{-1}$],
ρ_p = Density of soil particles [$kg\,m^{-3}$].

The transfer rate from top soil to deep soil, λ_{top_deep} [y^{-1}], is described by the following equation:

$$\lambda_{top\_deep} = \frac{Runoff + F_{ds,sa}}{\varepsilon_{ds} \cdot D_{ds}} R_f + \frac{BioT}{(1-\varepsilon_{ds}) \cdot \rho_p \cdot D_{ds}} \qquad \text{Equation A-18}$$

where
$F_{ds,\,sa}$ = Downward flow [$m^3\,m^{-2}\,y^{-1}$],
Runoff [$m^3\,m^{-2}\,y^{-1}$],
ε_{ds} = Porosity in deep soil [$m^3\,m^{-3}$],
D_{ds} = Depth of deep soil [m],
R_f = Retention, see above [–],
$BioT$ = Bioturbation, (transport of soil by earthworms) [$kg\,m^{-2}\,y^{-1}$],
ρ_p = Density of soil particles [$kg\,m^{-3}$].

Soil Erosion

There is a loss of elements due to erosion or removal of soil during agricultural practices. Geographical conditions, soil types and meteorological parameters such as wind and rain influence the magnitude of erosion. The size and density of the soil particles are also of importance. Land covered with vegetation are less exposed to erosion since the roots bind the material and the plants may cover parts of the surfaces.

The loss of radionuclides due to erosion, $\lambda_{erosion}$ [y^{-1}], is estimated as:

$$\lambda_{erosion} = \frac{R_{rate}}{D_{ts}(1-\varepsilon_{ts})\cdot\rho_p}$$ Equation A-19

where

R_{rate} = Removal of soil [kg $m^{-2} \cdot y^{-1}$],

D_{ts} = Depth of top soil [m],

ε_{ts} = Porosity of soil in the top soil (plough layer) [$m^3\ m^{-3}$],

ρ_s = Density of soil particles [kg m^{-3}].

Ingestion

Doses via ingestion, D_{ing} [Sv y^{-1}], are calculated using the concentration in the food item, the consumption rate and element specific dose coefficients for ingestion:

$$D_{ing} = HC_i \cdot U_i \cdot DC_{ing}$$ Equation A-20

where

HC_i = Consumption rate for pathway i [kg or litre per y],

U_i = Concentration in foodstuff i [Bq per kg or litre] (expressions given below),

DC_{ing} = Dose coefficients for ingestion [Sv/Bq].

Human consumption of agricultural products is represented by five groups of food items, i.e. milk, meat, vegetables, root crops and cereals. Fish represent food from aquatic systems. Consumption of algae and fresh water crustacean is also possible to consider even though this is not adequate for the studied area. For each of these food items the concentration of radionuclides is calculated as follows.

Milk and meat

Transfer of radionuclides to milk and meat is based on cattle's intake of contaminated fodder, soil and water. The concentration in milk, U_{milk} [Bq l^{-1}], and meat, U_{meat} [Bq kg^{-1}], is estimated from:

$$U_{milk} = In \cdot F_{milk}$$ Equation A-21

$$U_{meat} = In \cdot F_{meat}$$ Equation A-22

where

In = Daily intake of radionuclides [Bq day^{-1}] (expression given below),

F = Element specific transfer coefficient for milk and meat, respectively [day l^{-1}, day kg^{-1}].

Cattle are assumed to eat three different kinds of fodder; concentrated fodder (here represented by cereals), grass (fresh when grazing on the pasturage and as hay, harvested from the pasturage, the rest of the year, here combined and simply called pasturage) and plants growing on the shore of a lake or watercourse (hereafter called water plants). Additionally, some inadvertent consumption of soil when grazing is assumed. Radionuclides may also be taken in through consumption of contaminated water. Pasturage and cereals are contaminated through root uptake and retention of radionuclides on vegetation surfaces whereas water plants are contaminated through their uptake and transpiration of contaminated water. Different uptake pathways are considered in the different models. The cattle's daily intake of radionuclides (In) is calculated as a sum of products:

$$In = MC_x \cdot UC_x \ldots. + MC_y \cdot UC_y$$ Equation A-23

where

$MC_{x/y}$ = Daily consumption of food item, water and soil, respectively [kg or l day^{-1}],

$UC_{x/y}$ = Concentration of radionuclides in food item, water and soil, respectively [Bq per kg or litre] (expressions given below).

The concentrations of radionuclides in water and soil are obtained from the dispersion models. The concentration of radionuclides in cereals that are used as concentrated fodder to cattle is assumed to have the same concentration as the cereals for human consumption, which is obtained according to the expression given below. In the agricultural land and mire models it is assumed that pasturage is grown on contaminated areas and radionuclides are transferred to the grass via root uptake. The concentration in pasturage, UC_p [Bq kg^{-1}], is calculated as:

$$UC_p = C_i \cdot RUF_p \qquad \text{Equation A-24}$$

where

C_i = Concentration of radionuclides in soil or peat [Bq kg^{-1}], from the dispersion model,

RUF_p = Root uptake factor for pasturage [(Bq kg^{-1} dw)/(Bq kg^{-1} dw)].

Considered pathways (X) for intake of radionuclides in cattle in different biosphere models.

Model	Water	Pasturage	Cereals	Water plants	Soil
Coastal	X			X	
Lake	X			X	
Agricultural land		X	X		X

The consumption of water plants from a contaminated receptor, UC_{wp} [Bq kg^{-1}], does also contribute to the contamination of milk and meat. As the cattle is assumed to graze only part of the year the uptake of radionuclides via this pathway depends on, among other things, the number of days that they spend on the shore line:

$$UC_{wp} = \frac{CG}{365} \cdot \frac{C_w \cdot TR \cdot GD \cdot 10^{-6} \cdot 24}{Y_{wp}} \qquad \text{Equation A-25}$$

where

CG = Cattle grazing period on shores [days y^{-1}],

C_w = Concentration of radionuclides in water [Bq m^{-3}] (radionuclides in suspended matter included), from the dispersion model,

TR = Transpiration of water plants [g m^{-2}·h^{-1}],

GD = Average time for water plant transpiration before animal's consumption [days y^{-1}],

Y_{wp} = Annual production of water plants [kg m^{-2}·y^{-1}].

Crops

Crops are represented by cereals, root crops and green vegetables. In the agricultural land and mire models it is assumed that these crops are grown on contaminated soil or peat and radionuclides are transferred to the vegetation via root uptake. The concentration in the crops, U_i [Bq kg^{-1}], is calculated as:

$$U_i = C_i \cdot RUF_i \qquad \text{Equation A-26}$$

where

C_i = Concentration of radionuclides in soil or peat [Bq kg^{-1} dw], from dispersion model,

RUF_i = Root uptake factor for crop i (see below)[(Bq kg^{-1} dw)/(Bq kg^{-1} ww)],

$i = c$ for cereals,

$i = r$ for root crops,

$i = v$ for vegetables.

In other models, i.e. the lake and well models, contamination may occur through irrigation with contaminated water. In the SAFE study irrigation of a garden plot where root crops and vegetables are grown are simulated. Root crops are then contaminated via root uptake as well as retention of radionuclides on vegetation surfaces and thereafter translocation to edible parts. As more radionuclides are supplied at each irrigation occasion the radionuclide concentration depends on the number of irrigation events. Root crops are harvested after the irrigation period and the radionuclides supplied during the season are added up. The expression for resulting concentration in root crop products, U_i [Bq kg^{-1}], is:

$$U_i = C_s \cdot RUF_R + \sum_{0}^{Nr_{IRR}} I \cdot TL \cdot C_w \qquad \text{Equation A-27}$$

where

C_s = Concentration of radionuclides in soil [Bq kg^{-1} dw] from the dispersion model,

RUF_R = Root uptake factors for root crops (soil to plant transfer factors) [(Bq kg^{-1} ww)/Bq kg^{-1} dw)],

Nr_{IRR} = Number of irrigation occasions [y^{-1}],

I = Remaining water on the vegetation after each irrigation occasion [m],

TL = Translocation from plant surface to edible parts of plant, [(Bq kg^{-1} ww)/(Bq m^{-2})],

C_w = Concentration of radionuclides in irrigation water [Bq m^{-3}], from the dispersion model.

Vegetables are also contaminated from root uptake and surface contamination due to retention of contaminated irrigation water. The harvest of green vegetables is assumed to occur during the whole growing period (180–200 days per year). Therefore the mean concentration of surface contamination during the period is calculated and used in the dose calculations. The expression for the resulting content of radionuclides in vegetables, U_v [Bq kg^{-1}], is:

$$U_v = C_s \cdot RUF_v + \frac{C_w}{Y_v} \cdot \frac{I}{t_{tot}} \cdot \sum_{Nr_{IRR}} \int_{0}^{t_n} e^{-\tau . t_n} dt \qquad \text{Equation A-28}$$

where

C_s = Concentration of radionuclides in soil [Bq kg^{-1} dw], from the dispersion model,

RUF_v = Root uptake factor for vegetables (soil to plant transfer factor) [(Bq kg^{-1} ww)/Bq kg^{-1} dw)],

C_w = Concentration of radionuclides in irrigation water [Bq m^{-3}], from dispersion model,

Y_v = Yield of vegetables [kg m^{-2}·y^{-1}],

I = Remaining water on the vegetation after each irrigation occasion [m],

t_{tot} = Irrigation period, fraction of year [y^{-1}],

Nr_{IRR} = Number of irrigation occasions per year [y^{-1}],

t_n = Time between last irrigation occasion and harvest [days],

$\tau = \ln 2 / T_{½w}$ where $T_{½w}$ = weathering half-life [day].

Food from aquatic systems

Food from aquatic systems is represented by fish. Concentrations of radionuclides in those organisms are obtained by use of bioaccumulation factors for edible parts of the fish relative to the total concentration in the water (i.e. the amounts of radionuclides in water and on suspended matter). In order to use available databases which often are based on empirical concentration ratios, the water includes here the radionuclide fraction associated with suspended matter (which usually is a minor fraction). The bioaccumulation factors are valid for steady-state conditions and implicitly consider all uptake paths from the ambient environment. The expression for estimating the content of radionuclides in fish, crustaceans and algae (U_i) is:

$$U_i = BAF_i \cdot C_w \qquad \text{Equation A-29}$$

where

BAF_i = Element specific bioaccumulation factor from water to edible parts of fish [(Bq/kg ww)/(Bq/l)]

C_w = Concentration of radionuclides dissolved and suspended in the ambient water [Bq l^{-1}]

Inhalation

Doses via inhalation, D_{inh} [Sv y^{-1}], are calculated using the concentration of radionuclides in the air, the inhalation rate, the exposure time and element specific dose coefficients for inhalation:

$$D_{inh} = C_a \cdot IH \cdot H_i \cdot DC_{inh} \qquad \text{Equation A-30}$$

where

C_a = Concentration of radionuclides in air [Bq m^{-3}],

IH = Inhalation rate [m^3 h^{-1}],

H_i = Exposure time [h y^{-1}],

DC_{inh} = Dose coefficients for inhalation [Sv Bq^{-1}].

Radionuclides in air emanate from three sources; dust in air from soil or peat resuspension and flue gases produced when peat is used as fuel in a household. Particles in air are assumed to have the same radionuclide concentration as soil. The concentration of radionuclides in air due to contaminated soil resuspension, $C_{a,s}$, is expressed by:

$$C_{a,s} = C_s \cdot S \qquad \text{Equation A-31}$$

where

C_s = Concentration of radionuclides in soil [Bq kg^{-1} dw],

S = Dust content in air [kg m^{-3}].

External exposure

Doses via external exposure from soil, D_{ext} [Sv y^{-1}], are calculated using the concentration of radionuclides in soil, the soil density, the exposure time and element specific dose coefficients for external exposure:

$$D_{ext} = C_i \cdot \rho_i \cdot H_i \cdot DC_{ext} \qquad \text{Equation A-32}$$

where

C_i = Concentration of radionuclides in soil [Bq kg^{-1} dw],

ρ_i = Soil density [kg m^{-3}],

H_i = Exposure time [h y^{-1}],

DC_{ext} = External dose coefficients [(Sv h^{-1})/(Bq m^{-3})].